SUPPLEMENTARY MATERIAL

Mass spectrometric identification and structural analysis of the third generation synthetic cannabinoids on the UK market since the 2013 legislative ban

Lubertus Bijlsma[1,*], María Ibáñez[1,*], Bram Miserez[2], Solomon Ting Fung Ma[2], Trevor Shine[2], John Ramsey[2], Félix Hernández[1]

1. Research Institute for Pesticides and Water, University Jaume I, Avda. Sos Baynat, E-12071 Castellón, Spain.
2. TICTAC Communications Ltd., St George's University of London, Cranmer Terrace, London, SW17 0RE, UK

** Co-first authors*

Corresponding author: bijlsma@uji.es *Tel.: +34 964 387366 Fax: +34 964 387368*

UHPLC-QTOF MS

Instrumentation An Acquity Ultra-Performance Liquid Chromatography UPLC system (Waters, Milford, MA, USA) was interfaced to a hybrid quadrupole-orthogonal acceleration-TOF mass spectrometer (QTOF XEVO G2, Waters Micromass, Manchester, UK), using an orthogonal Z-spray-ESI interface operating in positive ion mode. The chromatographic separation was performed using an Acquity UPLC BEH C18 analytical column 100 × 2.1 mm with 1.7 µm particle size (Waters) at a flow rate of 300 µL/min. The mobile phases used were A = H2O and B = MeOH, both with 0.01% HCOOH. The initial percentage of B was 10%, which was linearly increased to 90% in 14 min, followed by a 2 minute isocratic period and then returned to initial conditions during 2 minutes. The total run time was 18 minutes. Nitrogen was used as drying- and nebulizing gas. The desolvation gas flow rate set at 1000 L/h. TOF-MS resolution was approximately 25,000 at full width half maximum (FWHM) at m/z 556. MS data were acquired over an m/z range of 50–1000 Da. A capillary voltage of 0.7 kV and cone voltage of 20 V were used. Collision gas was argon 99.995% (Praxair, Valencia, Spain). The desolvation temperature was set to 600 ºC and the source temperature to 135 ºC. The column temperature was set to 40 ºC. The injection volume was 2 µL.

For MSE screening experiments, two acquisition functions with different collision energies were created: the low energy (LE) function, selecting a collision energy of 4 eV, and the high energy (HE) function, with a collision energy ramp from 15 to 40 eV. For MS/MS experiments, five acquisition functions with different collision energies (from 10 to 50 eV) were created. For the unknown cannabinoids, additional experiments were performed from 50 to 100 eV. For further details, see [1].

[1] M. Ibáñez, L. Bijlsma, A.L. van Nuijs, J.V. Sancho, G. Haro, A. Covaci, F. Hernández, Quadrupole-time-of-flight mass spectrometry screening for synthetic cannabinoids in herbal blends. J. Mass Spectrom. 48 (2013) 685-694.

LC–QTOF-MS (/MS) identification of synthetic cannabinoids

Cannabinoids containing an adamantyl group linked by an amide and SDB-006

This group of cannabinoids includes APICA, 5F-APICA, APINACA and 5F-APINACA, all of which have an adamantyl group linked to the core by an amide bond. The core can be an indazole (APINACA and 5F-APINACA) or indole (APICA and 5F-APICA) and the tail a pentyl (APINACA and APICA) or a 5-fluoropentyl (5F-APICA and 5F-APINACA) chain (Fig. 1).

In all four compounds, the most abundant product ion at 30 eV corresponded to the adamantyl group (ion C, *m/z* 135.1174, $C_{10}H_{15}$) (Fig. 2a). Table 1 shows the product ions as well as the corresponding elemental compositions for all cannabinoids included in this group. Additionally, minor product ions at *m/z* 232.1138 and 214.1232 were observed for 5F-APICA and APICA respectively, corresponding to the loss of the amino-adamantly structure ($C_{10}H_{17}N$). At higher collision energies (50 eV), other product ions were observed corresponding to C_8H_{11} (ion D, *m/z* 107.0861), C_7H_9 (ion E, *m/z* 93.0704) and C_6H_7 (ion F, *m/z* 79.0548).

Regarding SDB-006 (*m/z* 321.1967), the one resulting from the breaking of the central amide (*m/z* 214.1232) and that corresponding to the pentyl indole group (*m/z* 188.1439) are the most abundant ions (Fig. 2b; Table 1). The *m/z* 144.0449 (also present in GC spectra) is inherent to the indole core, however it does not appear in the spectra of APICA and 5F-APICA. The tropilium ion at *m/z* 91.0548 is a proof of the end group, which is a toluene group.

LC–QTOF-MS(/MS) spectra at different collision energies for all cannabinoids Figs. S.1-S.5.

Cannabinoids with a quinolinyl ester, NM-2201 and 5F-MN-18

Five cannabinoids belong to this group of compounds containing a quinolinyl ester: PB-22, 5F-PB-22, BB-22, 5F-NPB-22, and FUB-PB-22. In addition, two related cannabinoids (NM-2201 and 5F-MN18) were also detected and are discussed here. Conversely, FUB-PB-22 will be discussed as a cannabinoid with a para-fluorotoluene chain as the mass spectra are quite similar.

For PB-22, 5F-PB-22, BB-22 and 5F-NPB-22, the main product ion (B) was formed by cleavage of the ester bond (Table 2). NM-2201 is structurally similar to these cannabinoids; the only difference is the naphthalene group instead of a quinolinyl group. 5F-MN-18, which is closely related to NM-2201, has an amide linkage. This resulted in a similar fragmentation pattern. The main ion (B) corresponded to *m/z* 214.1232 for PB-22 (N-pentyl-3-carbonyl-indole, Fig. 3a), 232.1138 for 5F-PB-22 and NM-2201 (N-(5-fluoro-pentyl)-3-carbonyl-indole), 240.1388 for BB-22 (N-methylcyclohexyl-3-carbonyl-indole), and 233.1090 for 5F-NPB-22 (Fig. 3b) and 5F-MN-18 (N-(5-fluoro-pentyl)-8-carbonyl-indazole). Another important product ion (E) was observed for PB-22, 5F-PB-22, BB-22 and NM-2201 at *m/z* 144.0449 (C_9H_6NO) and a minor ion (F) at *m/z* 116.0500 (C_8H_6N, corresponding to the indole group), was observed after CO loss from *m/z* 144 (Fig.3a). Similarly, for 5F-NPB-22 and 5F-MN-18, the product ions E and F corresponded to *m/z* 145.0402 ($C_8H_5N_2O$, due to the presence of an indazole group instead of an indole and 117.0453 ($C_7H_5N_2$, corresponding to the indazole group itself, this is, CO loss from 145), respectively (Fig. 3b). Additionally, for 5F-NPB-22 and 5F-MN-18 the *m/z* 213.1028 (ion C) was observed, corresponding to the loss of hydrogen fluoride (HF) from 233 (Figs. S.6-S.11).

Cannabinoids with a branched end group

Most cannabinoids have a ring structure as an end group (naphthalene, quilolinyl, adamantyl, etc.), but nine new cannabinoids from this study have a branched side chain: ADB-PINACA, AB-PINACA, 5F-AB-PINACA, 5F-Cumyl-PINACA, AB-CHMINACA, MDMB-CHMICA, and 5F-AMB as well as AB-FUBINACA and ADB-FUBINACA (Fig. 1). The latter two will be discussed in a separate section together with the cannabinoids containing a *para*-fluorotoluene chain.

For the four cannabinoids containing the N-1-amino-3-methyl-1-oxobutan-2-yl group, an initial product ion was observed corresponding to the loss of NH_3 (ion B), at *m/z* 328.2025, 314.1869, 332.1774 and 340.2025 for ADB-PINACA, AB-PINACA, 5F-AB-PINACA (Fig. 4b) and AB-CHMINACA, respectively. Subsequently, the loss of CO (ion C) from this ion, was observed at *m/z* 300.2076 for ADB-PINACA (Fig. 4a), 286.1919 for AB-PINACA, 304.1825 for 5F-AB-PINACA, and 312.2076 for AB-CHMINACA (Table 3). In the case of 5F-AMB an initial product ion was observed due to the loss of methanol (*m/z* 332.1774) followed by the loss of CO (m/z 304.1825) (Table 3).

The most prominent product ions in all spectra were the result of the cleavage of the central amide bond (ion D), *m/z* 215.1184 for ADB-PINACA and AB-PINACA, 233.1090 for 5F-AB-PINACA (Fig. 4b), 5F-Cumyl-AKB48 analog and 5F-AMB, 241.1341 for AB-CHMINACA, and 240.1388 for MDMB-CHMICA (Table 3). The *m/z* 145.0398 (G) is present in all spectra ($C_8H_5N_2O$) resulting from the double cleavage of the carbonyl-indazole group (except *m/z* 144.0441 for MDMB-CHMINACA due to the indole group, C_9H_6NO). Moreover, for the compounds containing a fluorine atom, a subsequent HF loss was also observed (ion E), at *m/z* 213.1028 for 5F-AMB, 5F-AB-PINACA and the cumyl derivative of 5F-AKB48 (5F-Cumyl-PINACA). For these three

compounds, the product ion *m/z* 177.0463 (ion F), corresponding to the pentyl-indazole group, was also observed (Figs. S.12-S.18).

Cannabinoids with a *para*-fluorotoluene chain

AB-FUBINACA, ADB-FUBINACA and FUB-PB-22 all have a *para*-fluorotoluene side chain (Figs. 1, 5). For AB-FUBINACA and ADB-FUBINACA (also containing the N-1-amino-3-methyl-1-oxobutan-2-yl substituent), product ions corresponding to an initial loss of NH_3 (*m/z* 352.1461 and 366.1618, respectively) and the subsequent CO loss (*m/z* 324.1512 and 338.1669, respectively) were observed (Table 4). At higher collision energies, AB-FUBINACA, ADB-FUBINACA and FUB-PB-22 showed two abundant product ions. The first was the result of the cleavage of the central amide bond (ion D) at *m/z* 253.0777 for AB-FUBINACA and ADB-FUBINACA or of the ester at *m/z* 252.0825 for FUB-PB-22. The second at *m/z* 109.0454 (ion E, C_7H_6F), was due to the presence of the *para*-fluorotoluene side chain (Table 4; Figs. S.19-S.21).

Cannabinoids with two chromatographic peaks

Two chromatographic peaks were observed in the LC–QTOF-MS chromatograms at the expected *m/z* for some compounds, concretely for ADB-PINACA, AB-PINACA, 5F-AB-PINACA, AB-CHMINACA and AB-FUBINACA (Table 3; Fig. 5a). For all of the five compounds, these two chromatographic peaks presented different fragmentation, all being compatible with the structure of the corresponding cannabinoid. All of them possess a terminal amino group and an enantiomeric carbon at the linker part. Moreover, some common product ions were also observed but with different relative intensities. As an example, Figs S.5(B-C) show the MS/MS spectra for the two chromatographic peaks obtained for AB-FUBINACA. Note the presence of product ions at *m/z* 244, 216 and 145

in Fig. S.5B (corresponding to the chromatographic peak at 11.07) and its absence in Fig. S.5C (peak at 11.53 min). Moreover, in all cases, the first chromatographic peak presented an abundant protonated molecule whereas the second presented as peak base at 10 eV with the product ion corresponding to the loss of NH_3. This does not happen in GC–MS, where only one chromatographic peak was observed. This might be explained by the occurrence of rotamers.

Cannabinoids with a carbonyl link

THJ-018 and THJ-2201 have similar structures, differing only in the presence of a fluorine atom at the end of the chain in THJ-2201. The main product ions were at *m/z* 215.1184 for THJ-018 and 233.1090 for THJ 2201, obtained after loss of naphthalene group ($C_{10}H_8$) (see Table 5). In the case of THJ-2201 (Figs 6a), a subsequent loss of HF was also observed (*m/z* 213.1028). For both compounds, a fragment ion at *m/z* 145.0402 ($C_8H_5N_2O$) was also present. Three minor product ions were observed at *m/z* 127.0548 (corresponding to the naphthalene group itself, $C_{10}H_7$), 117.0453 ($C_7H_5N_2$, obtained after the CO loss from 145) and 90.0344 (C_6H_4N, corresponding to the loss of HCN from 117) (Figs S.22-S.23).

Regarding EG-018 (Fig. 6b) and BZ-2201, they present similar fragmentation (Table 5). The major product ions were *m/z* 155.0497 ($C_{11}H_7O$, corresponding to the carbonyl-naphtalene group) and 127.0548 (corresponding to the naphthalene group) (Figs S.24-S.25).

Unidentified novel synthetic cannabinoid

Unidentified compound 1

This compound was present in an herbal sample. It was initially investigated by GC–MS analysis. Most cannabinoids present the molecular ion in the EI spectrum, and it is only missing in the case that a branched side chain and a *para*-fluorotoluene group is present. As *m/z* 109 is missing, there is no *para*-fluorotoluene group and the ion at *m/z* 377 is most likely the molecular ion. The ions at *m/z* 144 and *m/z* 232 reveal the presence of a 5-fluoro-pentyl-indole-carbonyl group. The presence of the ion at *m/z* 145 can be confusing, but is the fluoro-quinoline group. The ions at *m/z* 145 and *m/z* 232 together form the molecular ion *m/z* 377. The *m/z* 302 is the result of the loss of the side chain (C_4H_8F). So, this compound seems to be a cannabinoid with a molecular mass of 377 that contains fluoro-pentyl-indole-carbonyl and a side chain with a mass of 145, which is uncommon (Fig. 7a).

Regarding LC information, the protonated molecule of the chromatographic peak at 13.38 min was found to be *m/z* 378.1670, which supports the hypothesis that the molecular ion was 377 as GC–MS analysis revealed. Its sodium adduct (*m/z* 400.1490) was also observed. After performing an elemental composition calculation, and considering the following parameters settings C(0-40), H(0-50), N(0-5), O (0-5) and F (0-2), two plausible elemental compositions were obtained within a ±5 ppm mass error: $C_{24}H_{22}NOF_2$ (expressed as protonated molecule, 0.3 ppm error) and $C_{27}H_{21}NF$ (3.2 ppm). Note that no bromine or chlorine atoms were considered as their typical isotopic profile was not observed in the spectra. After performing MS/MS experiments in an additional injection, the elemental composition of the unknown was restricted to at least 1 oxygen atom and 1 fluorine atom due to the HF and CO losses observed, as it is explained below. Therefore, the only possibility was $C_{24}H_{22}NOF_2$.

The MS/MS spectrum at 20 eV showed the presence of two product ions at *m/z* 232.1137 ($C_{14}H_{15}NOF$, -0.4 ppm) and 173.0402 ($C_{11}H_6OF$, -0.6 ppm) (Fig. 7b). At higher collision energies, a new product ion *m/z* 145.045 ($C_{10}H_6F$, 0 ppm) was observed due to the CO loss from m/z 173 (40eV). The product ion *m/z* 125.0391 ($C_{10}H_5$, 0 ppm) resulted from the HF loss from *m/z* 145 (60 eV) and 2 product ions were obtained at *m/z* 99.0233 (C_8H_3, -2 ppm) and 75.0233 (C_6H_3, 2.7 ppm) (100 eV). After studying this fragmentation and that observed for other cannabinoids, we suggest the compound to be F2201 (Fig. 7). This compound is not new (already administered as CAS 1391485-39-4), but it had never been seen on the drug market up to the moment of the analysis.

Unidentified compound 2

GC–MS analysis of another herbal sample showed two compounds: SDB-006 and an unknown substance. The molecular ion was *m/z* 250, this is 70 amu lower than SDB-006. Its EI spectrum presented fragments at *m/z* 144, 114, 91, and 77 in common with SDB-006, but lacking the main fragments at *m/z* 214 (pentyl-indole-carbonyl). The ion at *m/z* 144 is likely indole-carbonyl, thus lacking the pentyl chain. The 70 amu difference with SDB-006 is likely the pentyl side chain. The ions at *m/z* 91 and 77 are the tropilium ion and benzene group, respectively.

Regarding LC analysis, the protonated molecule of the chromatographic peak at 9 min was found to be *m/z* 251.1186. After performing an elemental composition calculation, and considering the following parameter settings C(0-40), H(0-50), N(0-5), O (0-5) and F (0-2), two plausible elemental compositions were obtained within a ±5 ppm mass error: $C_{16}H_{15}N_2O$ (0.8 ppm) and $C_{13}H_{16}N_2O_2F$ (-4 ppm), both expressed as a protonated molecule. Considering the high mass error obtained for the last candidate and

the absence of HF loss (typical in almost all cannabinoids containing a fluorine atom) the elemental composition $C_{16}H_{15}N_2O$ was finally proposed for this unknown.

In this case, the MS/MS spectra (Fig. 8) showed only three product ions at m/z 144.0451 (C_9H_6NO, 1.4 ppm), 116.0505 (C_8H_6N, 4.3 ppm) and 91.0556 (C_7H_7, -3.3 ppm). After studying this fragmentation and that observed for the other cannabinoids, we suggest the compound to be dealkyl-SDB006 (Fig. 8)

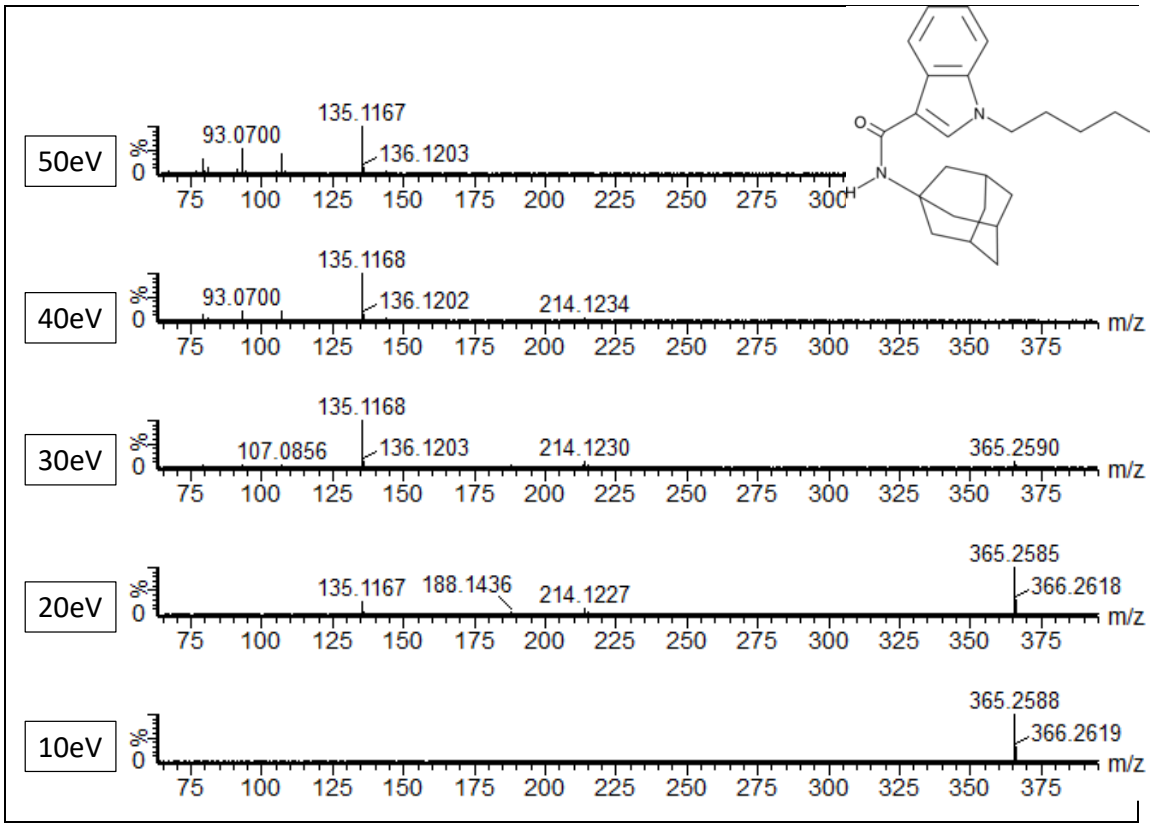

Figure S.1. UHPLC-QTOF MS/MS spectra at different collision energies (from bottom to top, 10, 20, 30, 40 and 50 eV) for APICA

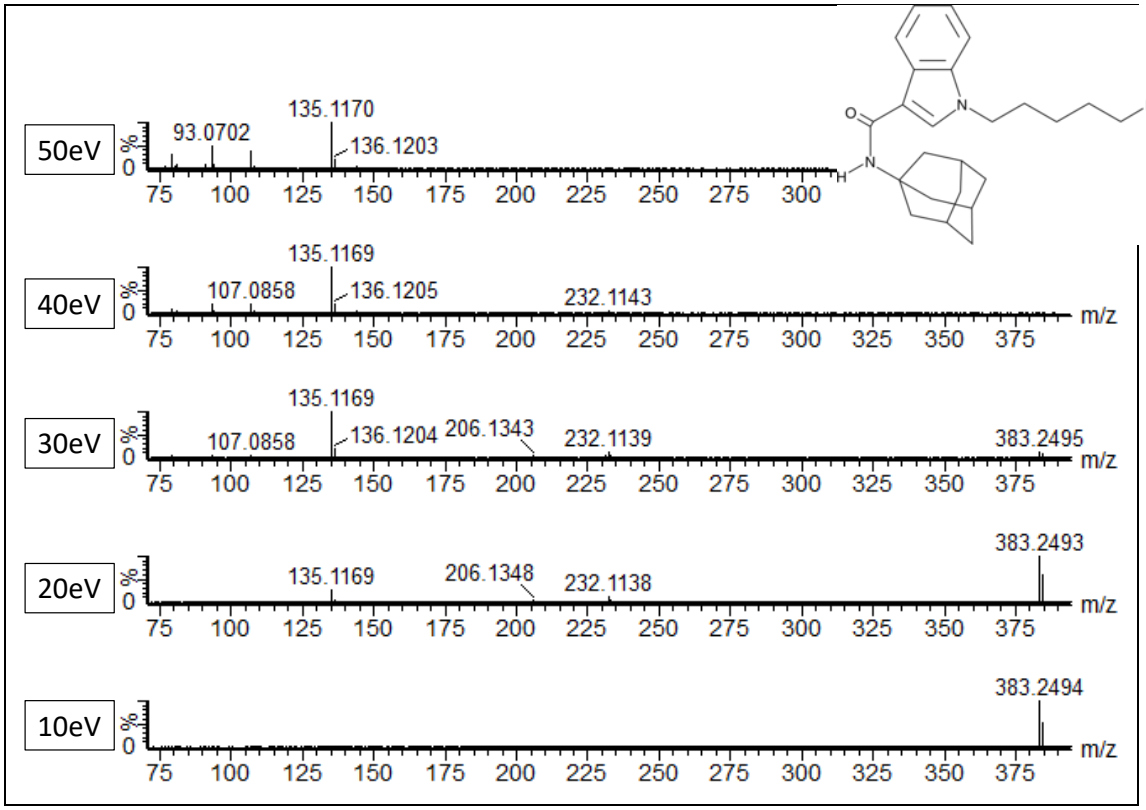

Figure S.2. UHPLC-QTOF MS/MS spectra at different collision energies (from bottom to top, 10, 20, 30, 40 and 50 eV) for 5F-APICA

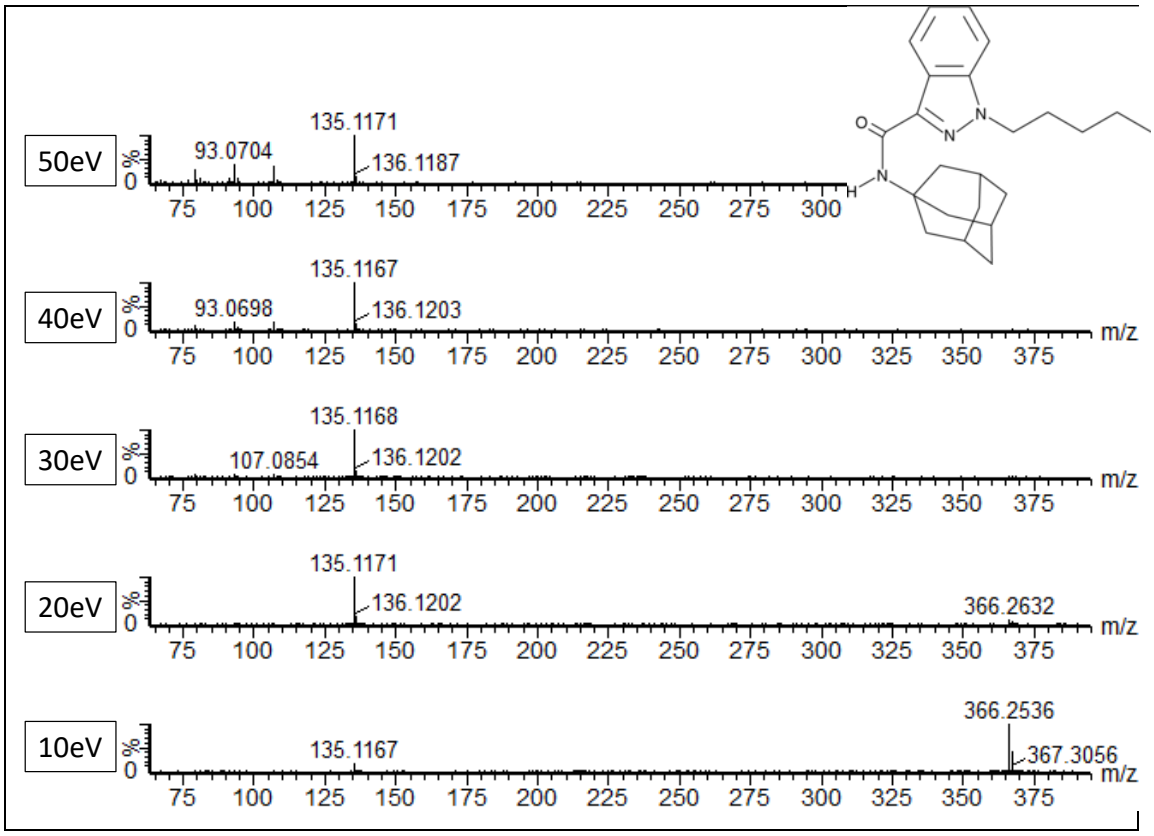

Figure S.3. UHPLC-QTOF MS/MS spectra at different collision energies (from bottom to top, 10, 20, 30, 40 and 50 eV) for APINACA

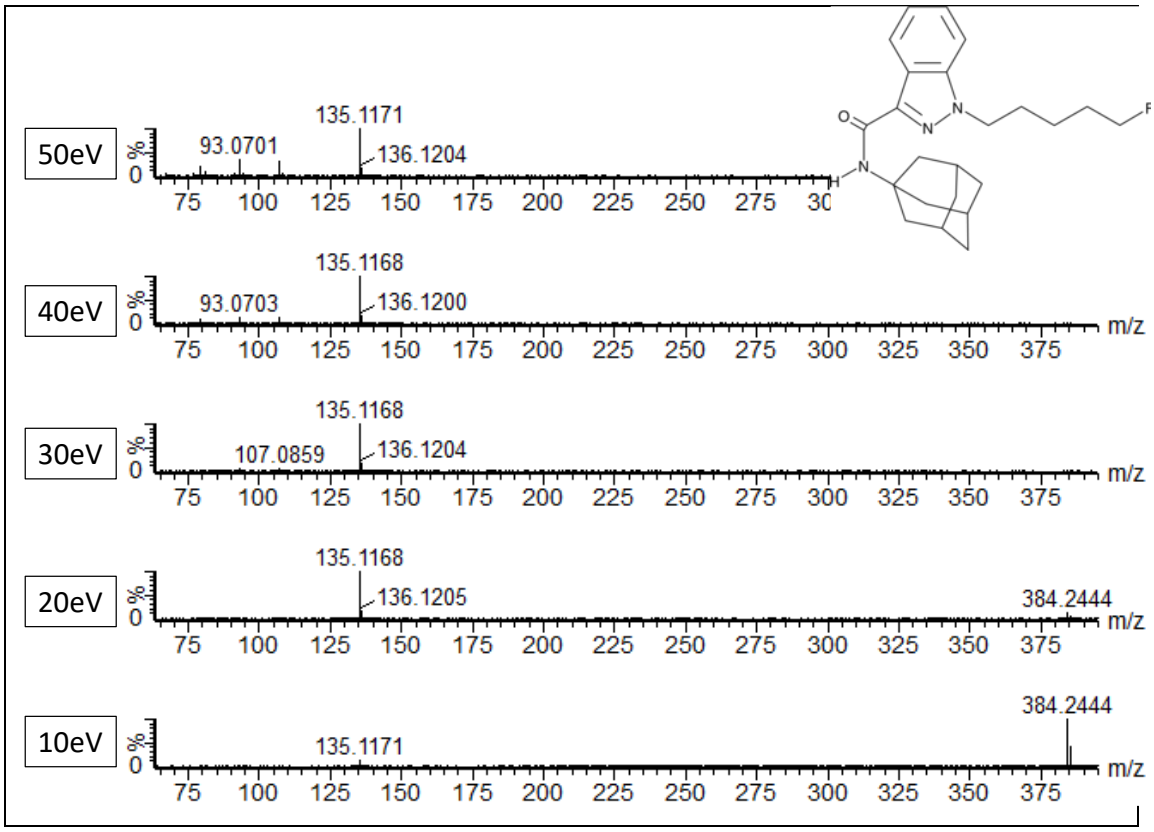

Figure S.4. UHPLC-QTOF MS/MS spectra at different collision energies (from bottom to top, 10, 20, 30, 40 and 50 eV) for 5F-APINACA

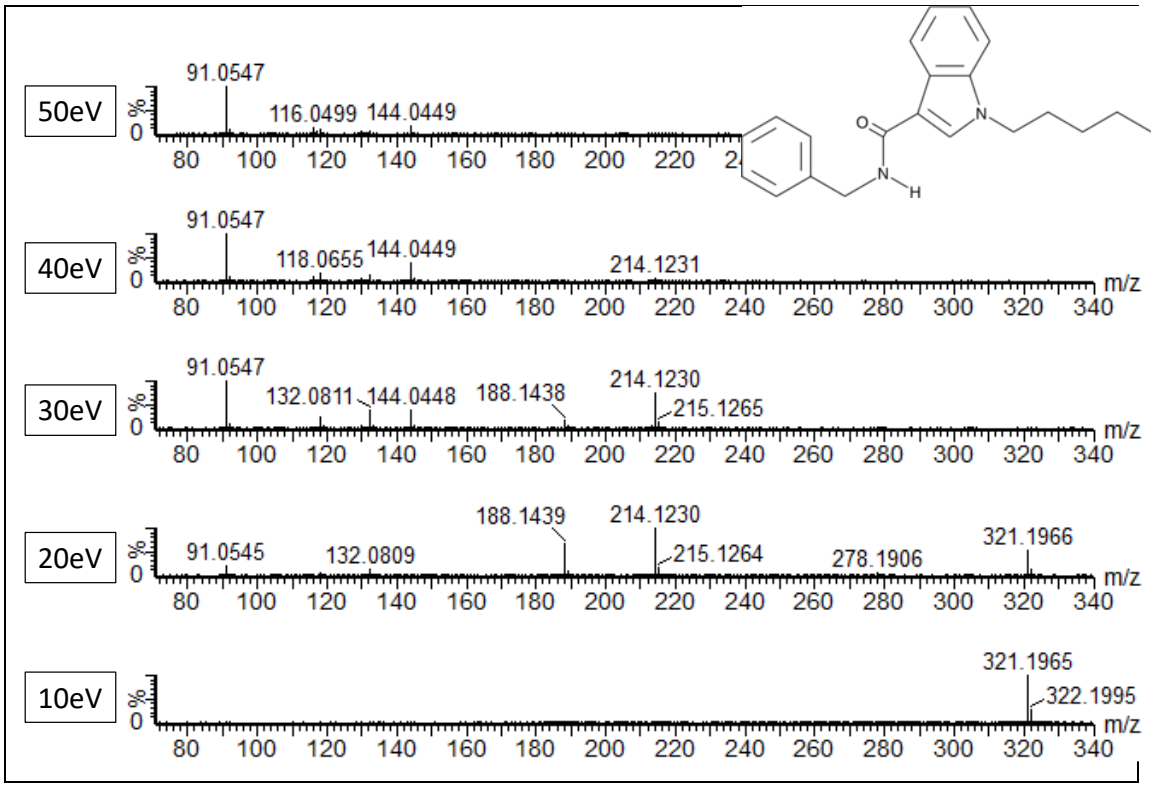

Figure S.5. UHPLC-QTOF MS/MS spectra at different collision energies (from bottom to top, 10, 20, 30, 40 and 50 eV) for SDB-006

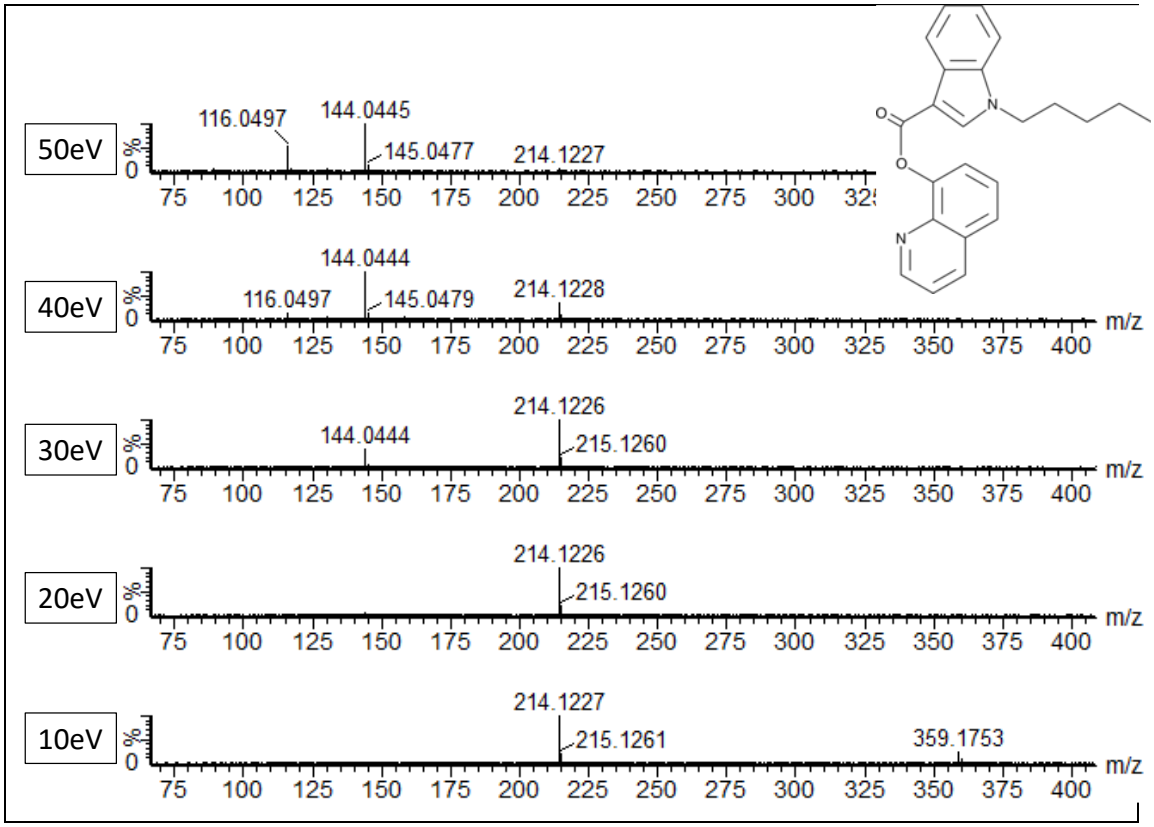

Figure S.6. UHPLC-QTOF MS/MS spectra at different collision energies (from bottom to top, 10, 20, 30, 40 and 50 eV) for PB-22

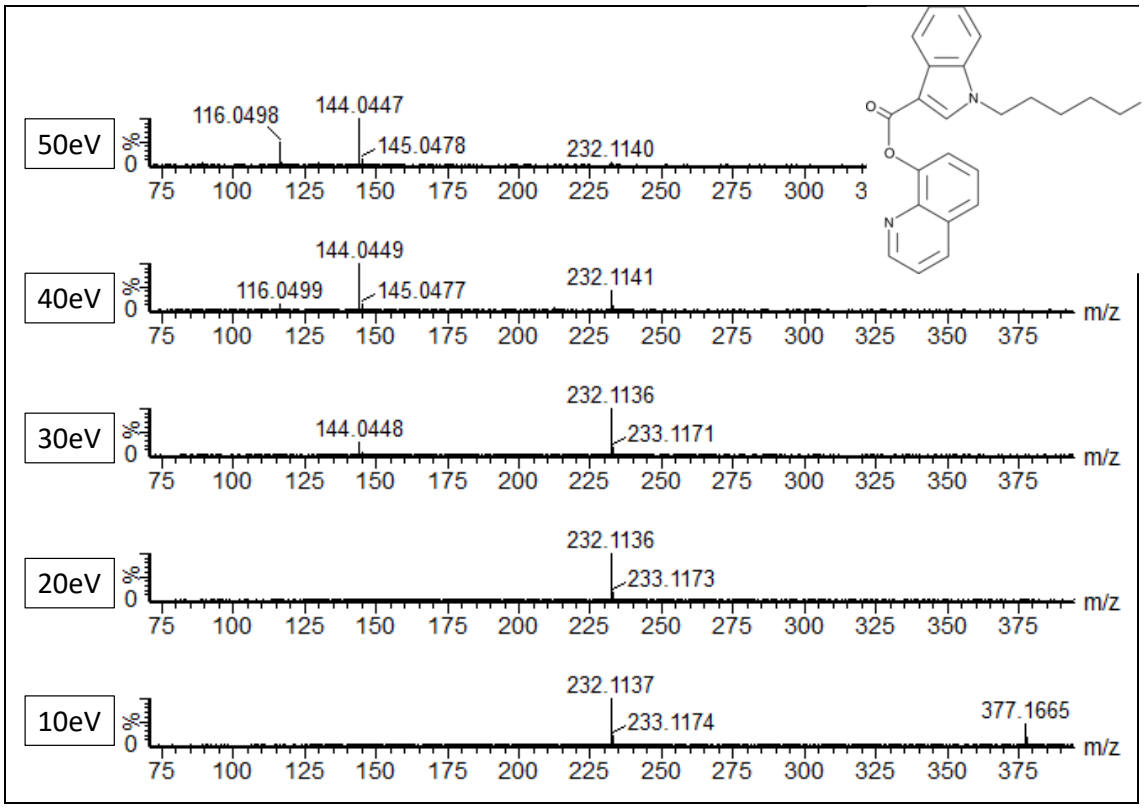

Figure S.7. UHPLC-QTOF MS/MS spectra at different collision energies (from bottom to top, 10, 20, 30, 40 and 50 eV) for 5F-PB-22

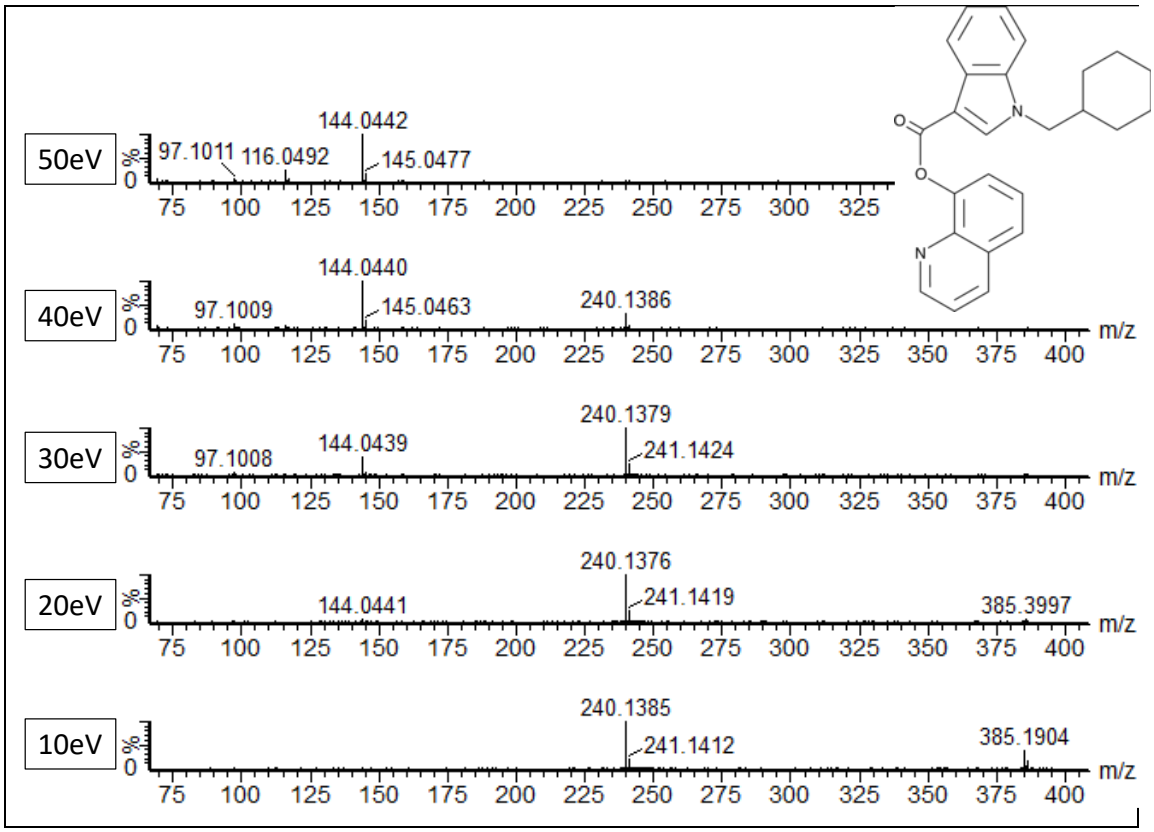

Figure S.8. UHPLC-QTOF MS/MS spectra at different collision energies (from bottom to top, 10, 20, 30, 40 and 50 eV) for BB-22

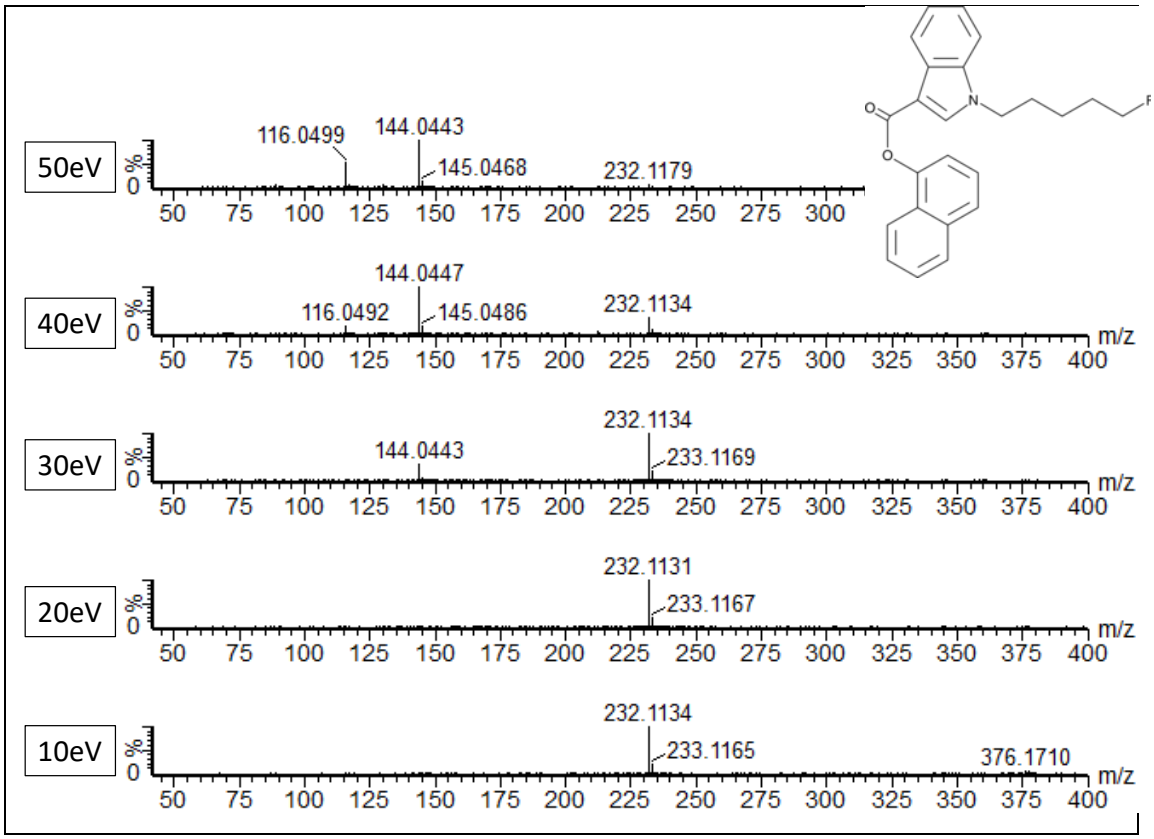

Figure S.9. UHPLC-QTOF MS/MS spectra at different collision energies (from bottom to top, 10, 20, 30, 40 and 50 eV) for NM-2201

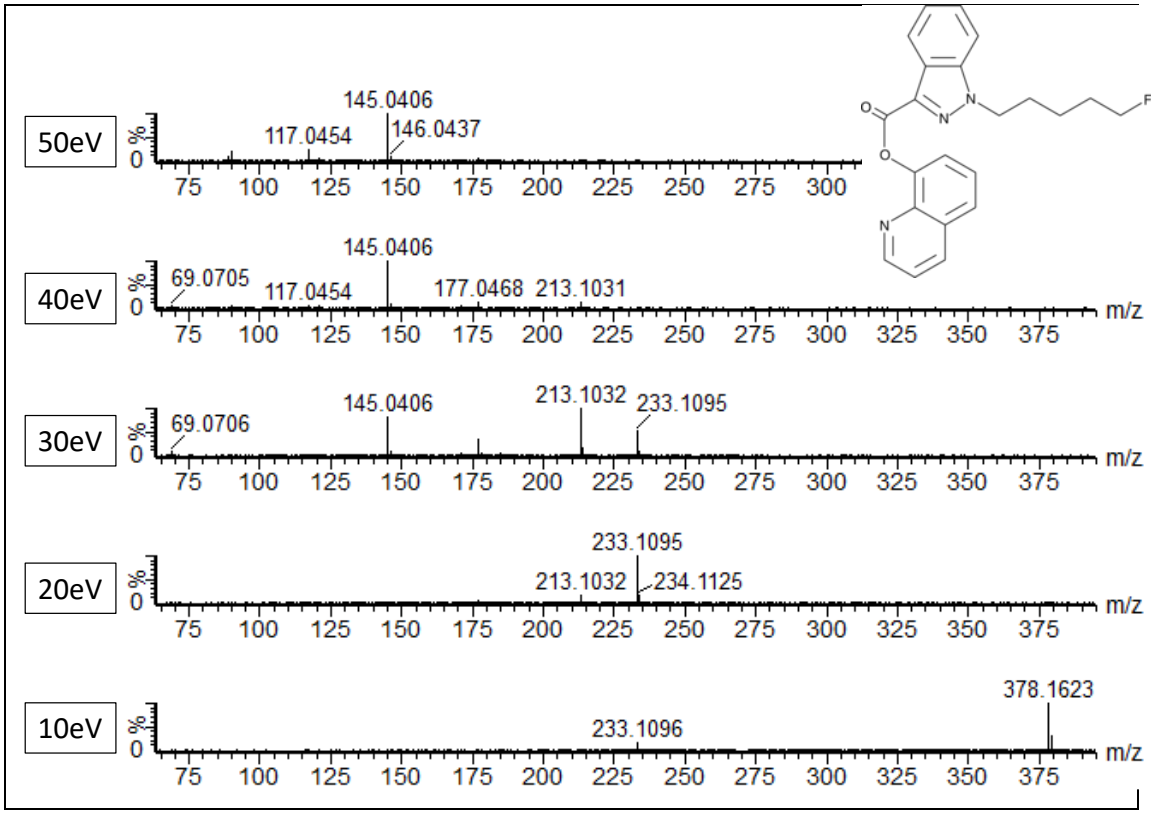

Figure S.10. UHPLC-QTOF MS/MS spectra at different collision energies (from bottom to top, 10, 20, 30, 40 and 50 eV) for 5F-NPB-22

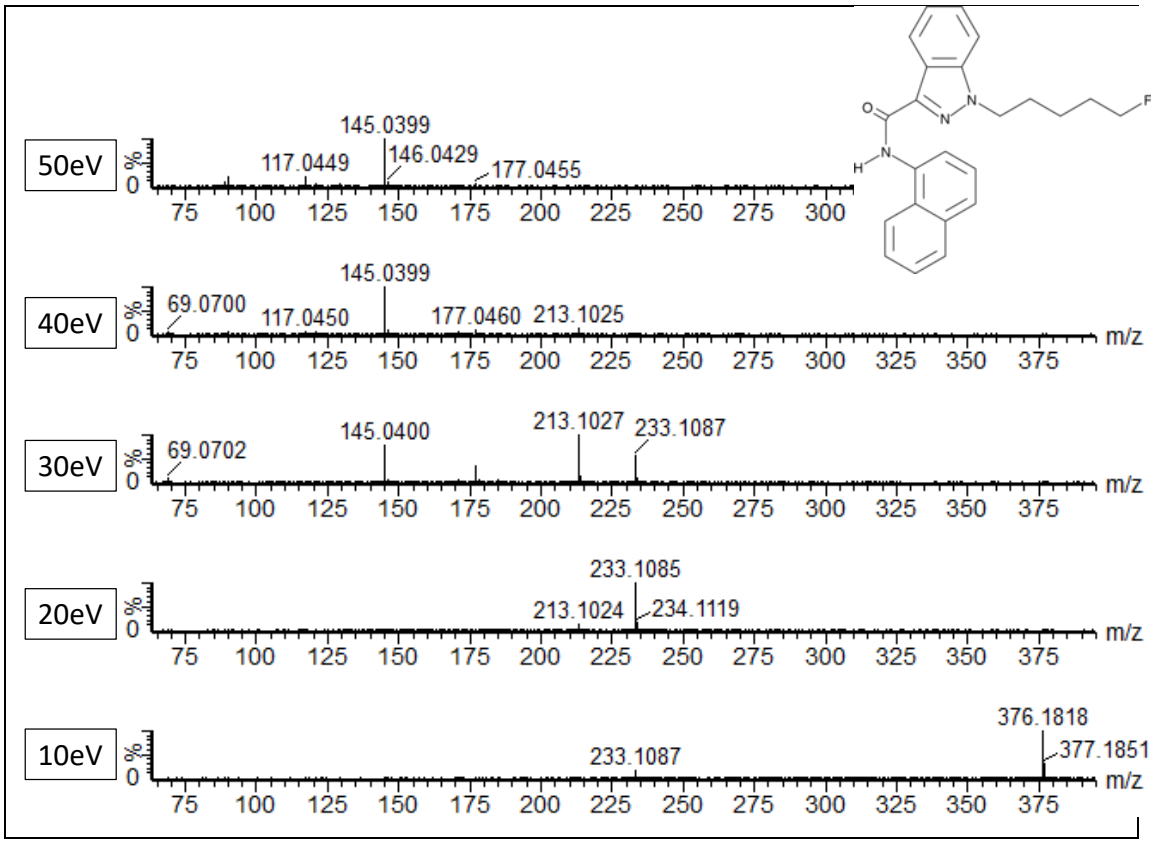

Figure S.11. UHPLC-QTOF MS/MS spectra at different collision energies (from bottom to top, 10, 20, 30, 40 and 50 eV) for 5F-MN-18

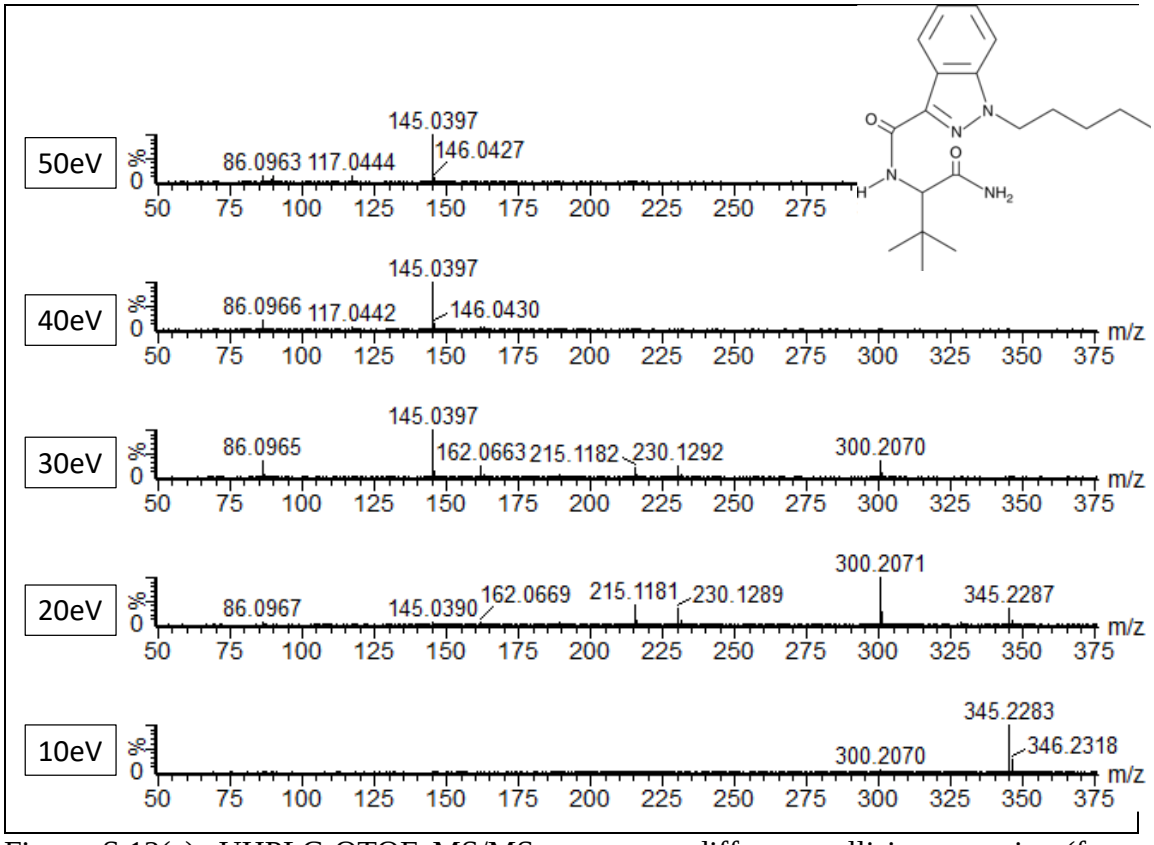

Figure S.12(a). UHPLC-QTOF MS/MS spectra at different collision energies (from bottom to top, 10, 20, 30, 40 and 50 eV) for ADB-PINACA (12,4 min)

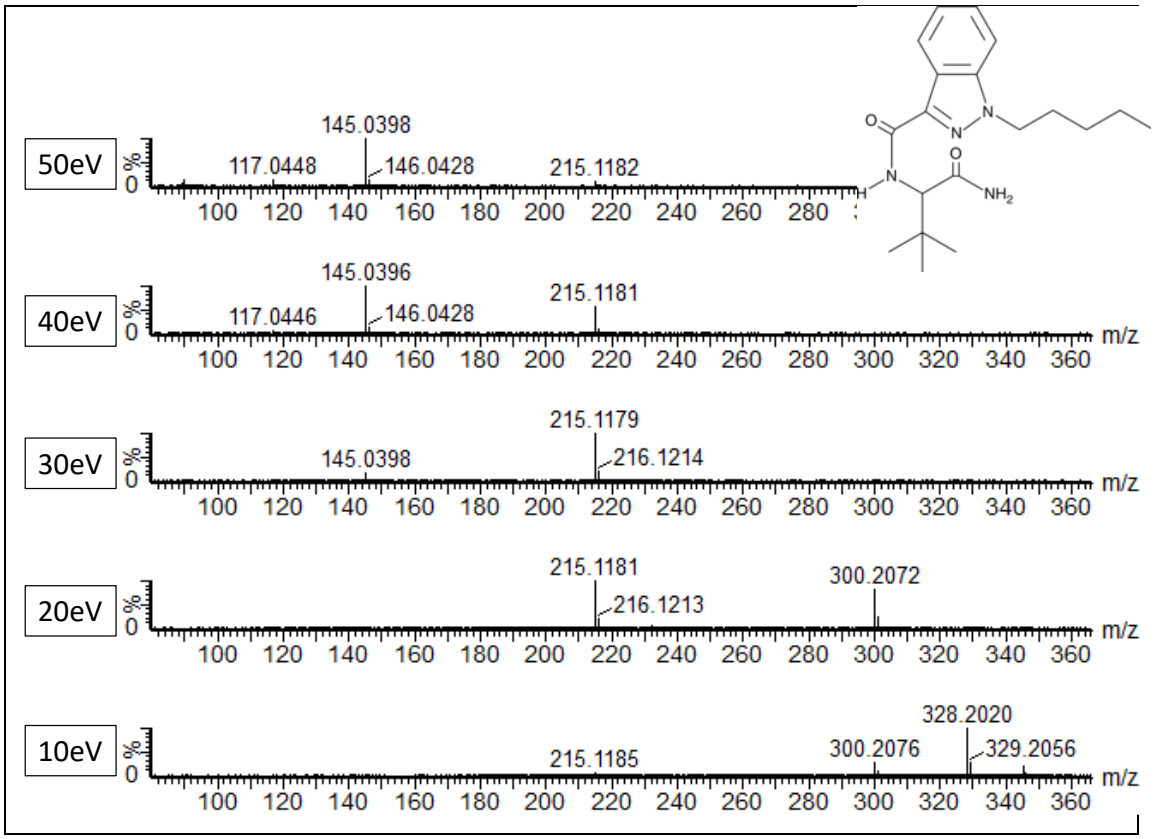

Figure S.12(b). UHPLC-QTOF MS/MS spectra at different collision energies (from bottom to top, 10, 20, 30, 40 and 50 eV) for ADB-PINACA (13.1 min)

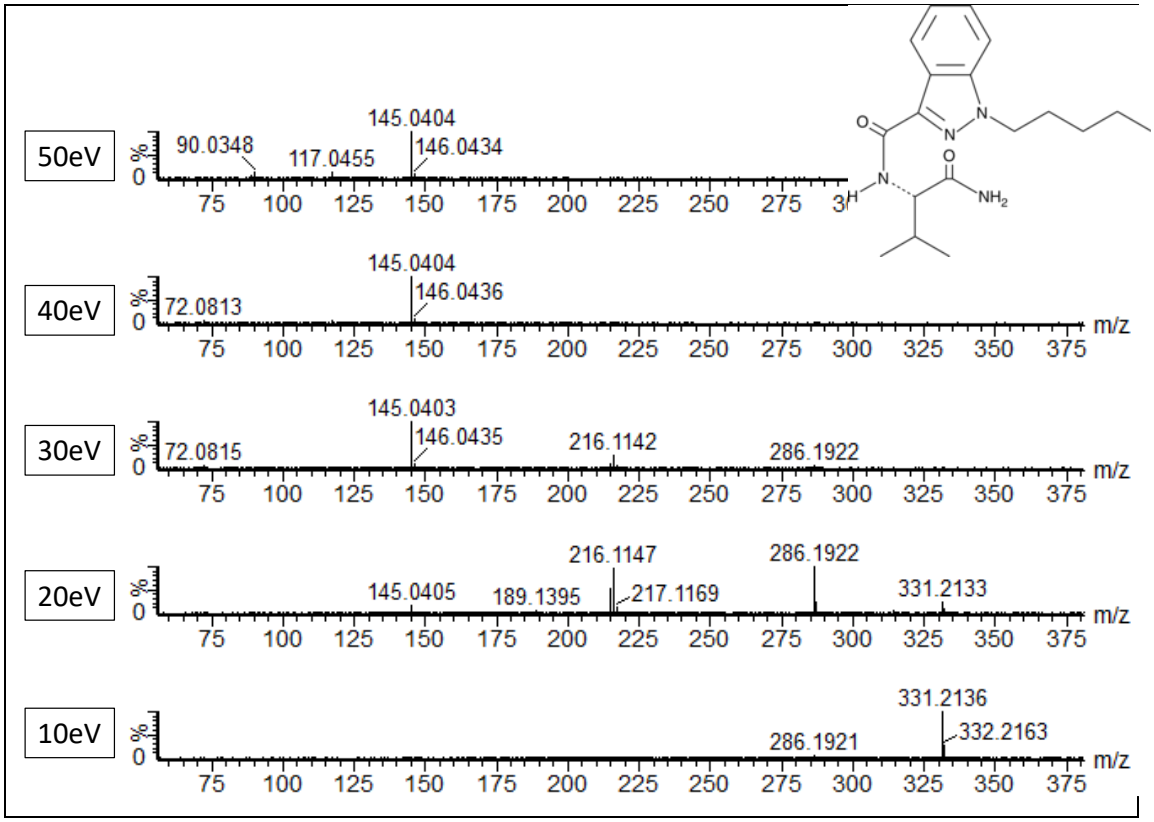

Figure S.13(a). UHPLC-QTOF MS/MS spectra at different collision energies (from bottom to top, 10, 20, 30, 40 and 50 eV) for AB-PINACA (11.3 min)

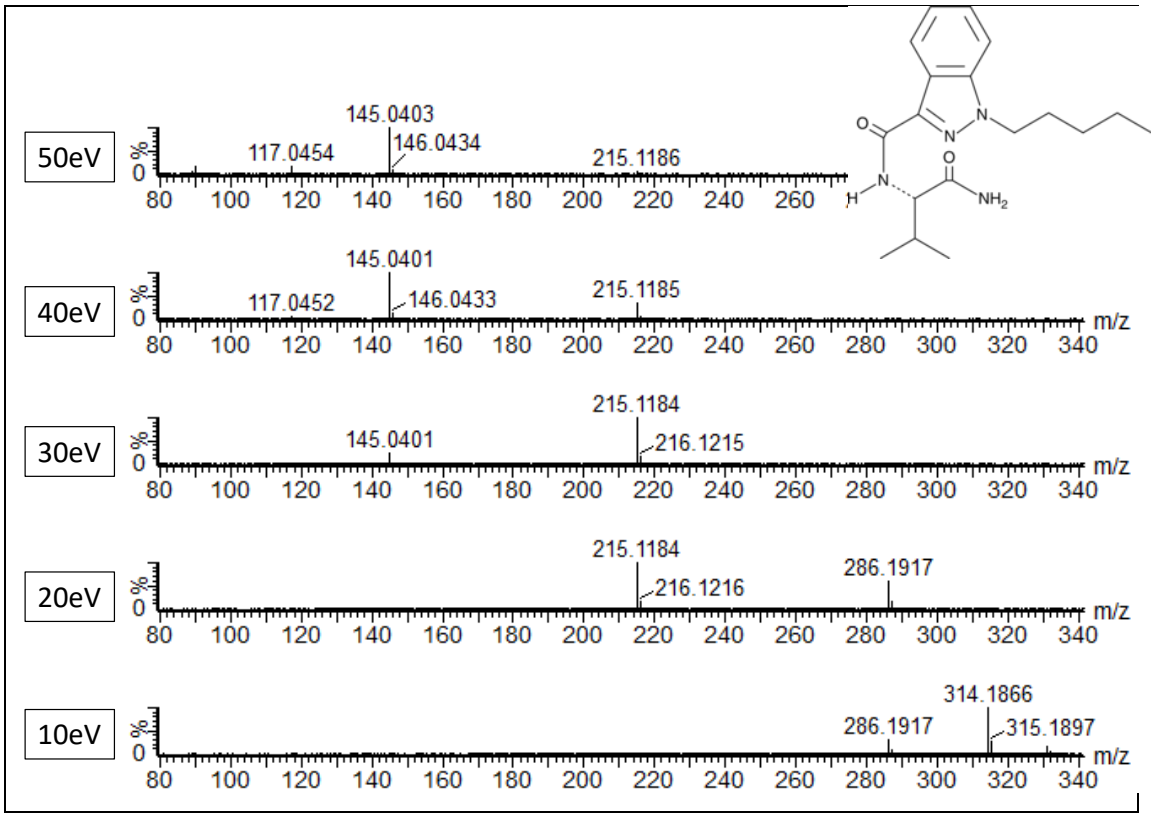

Figure S.13(b). UHPLC-QTOF MS/MS spectra at different collision energies (from bottom to top, 10, 20, 30, 40 and 50 eV) for AB-PINACA (12.2 min)

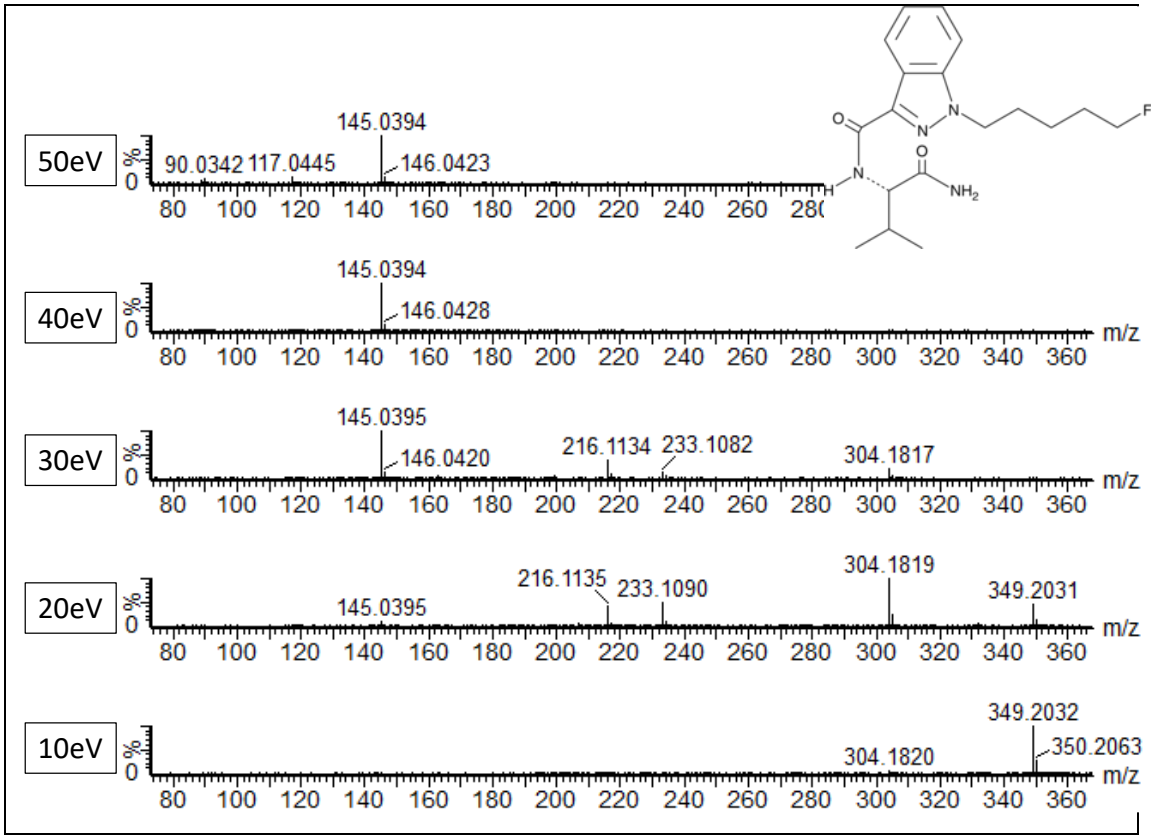

Figure S.14(a). UHPLC-QTOF MS/MS spectra at different collision energies (from bottom to top, 10, 20, 30, 40 and 50 eV) for 5F-AB-PINACA (10.35 min)

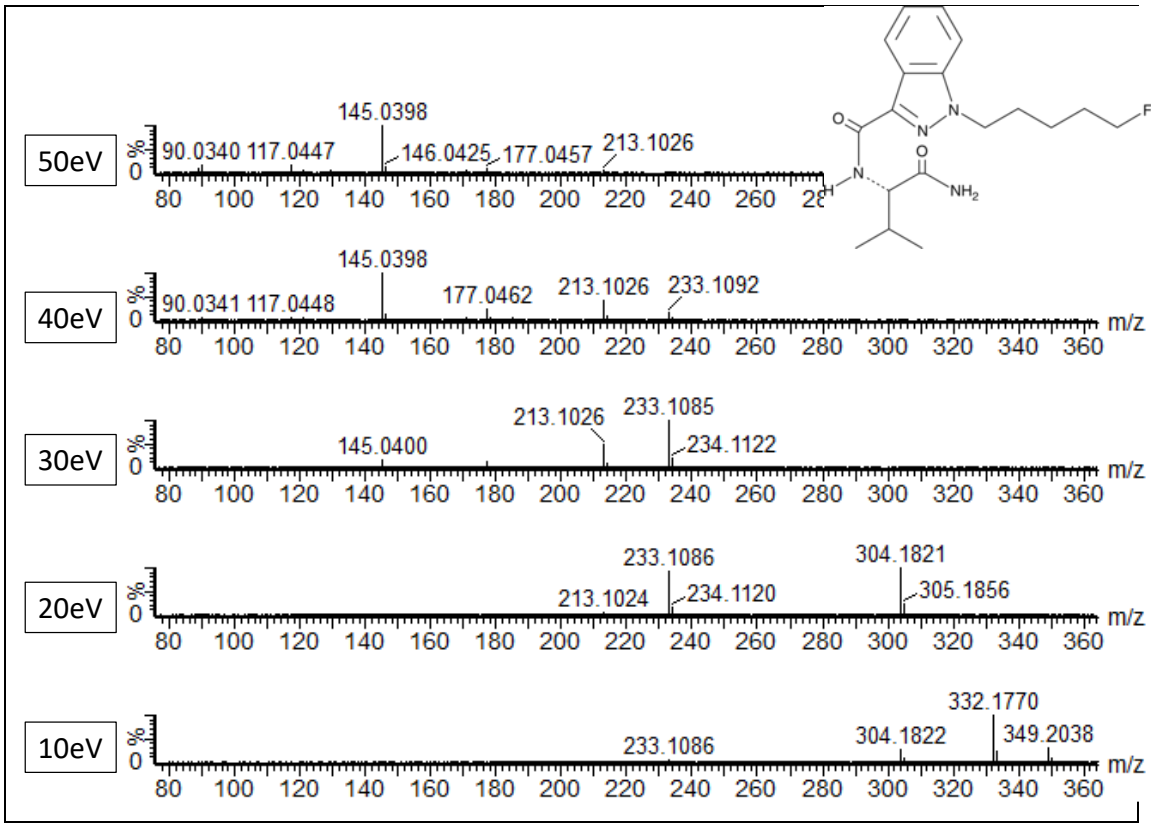

Figure S.14(b). UHPLC-QTOF MS/MS spectra at different collision energies (from bottom to top, 10, 20, 30, 40 and 50 eV) for 5F-AB-PINACA (11.02 min)

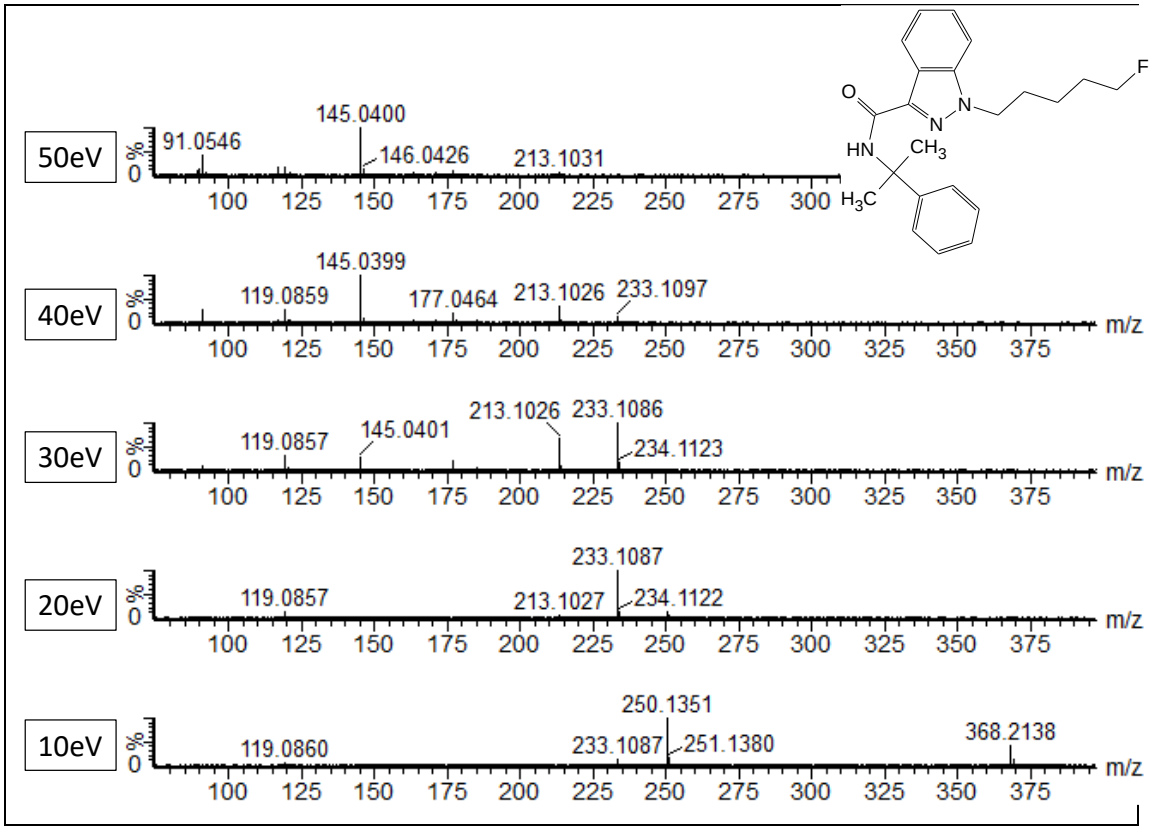

Figure S.15. UHPLC-QTOF MS/MS spectra at different collision energies (from bottom to top, 10, 20, 30, 40 and 50 eV) for 5F-cumyl-PINACA

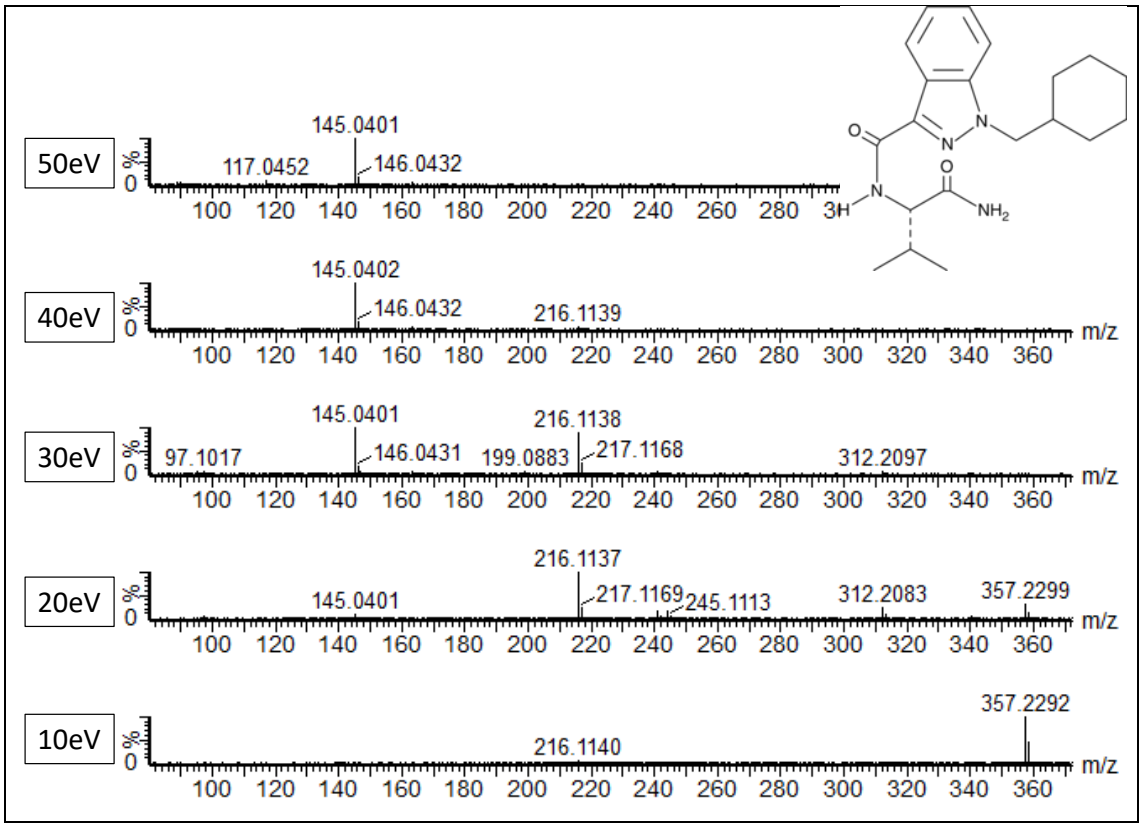

Figure S.16(a). UHPLC-QTOF MS/MS spectra at different collision energies (from bottom to top, 10, 20, 30, 40 and 50 eV) for AB-CHMINACA (12.1 min)

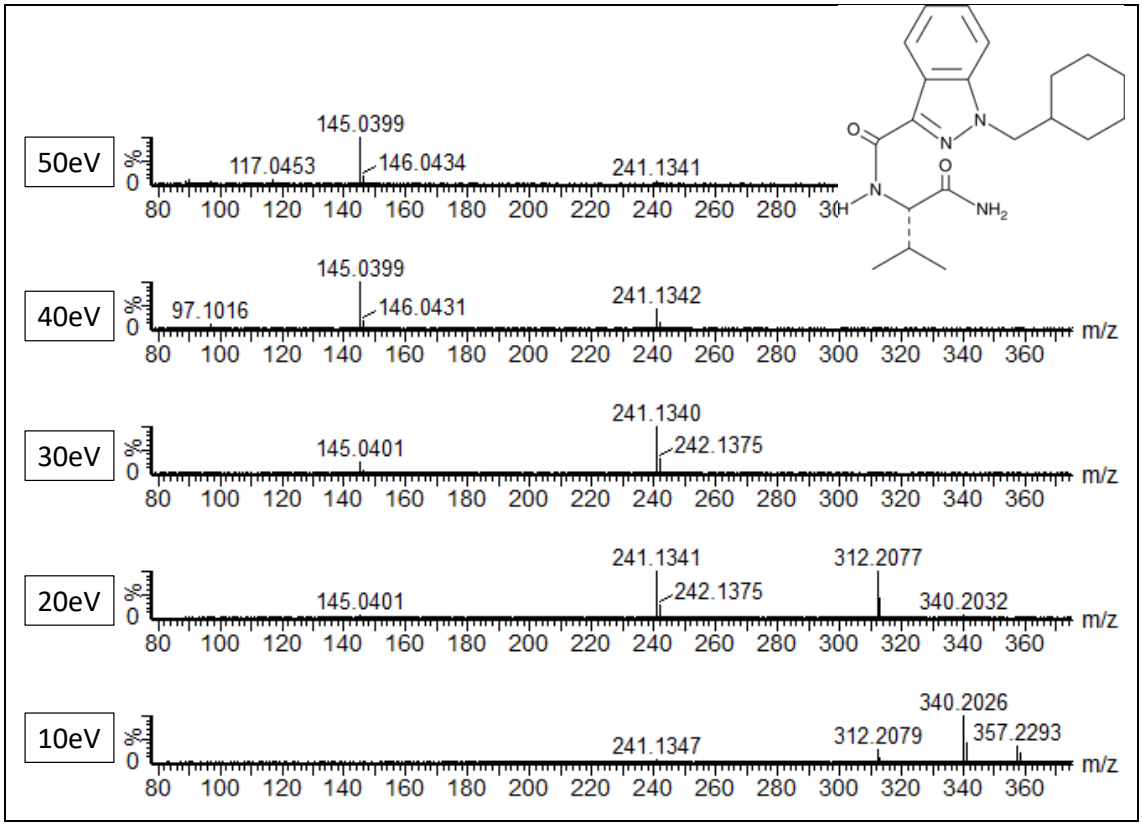

Figure S.16(b). UHPLC-QTOF MS/MS spectra at different collision energies (from bottom to top, 10, 20, 30, 40 and 50 eV) for AB-CHMINACA (13.1 min)

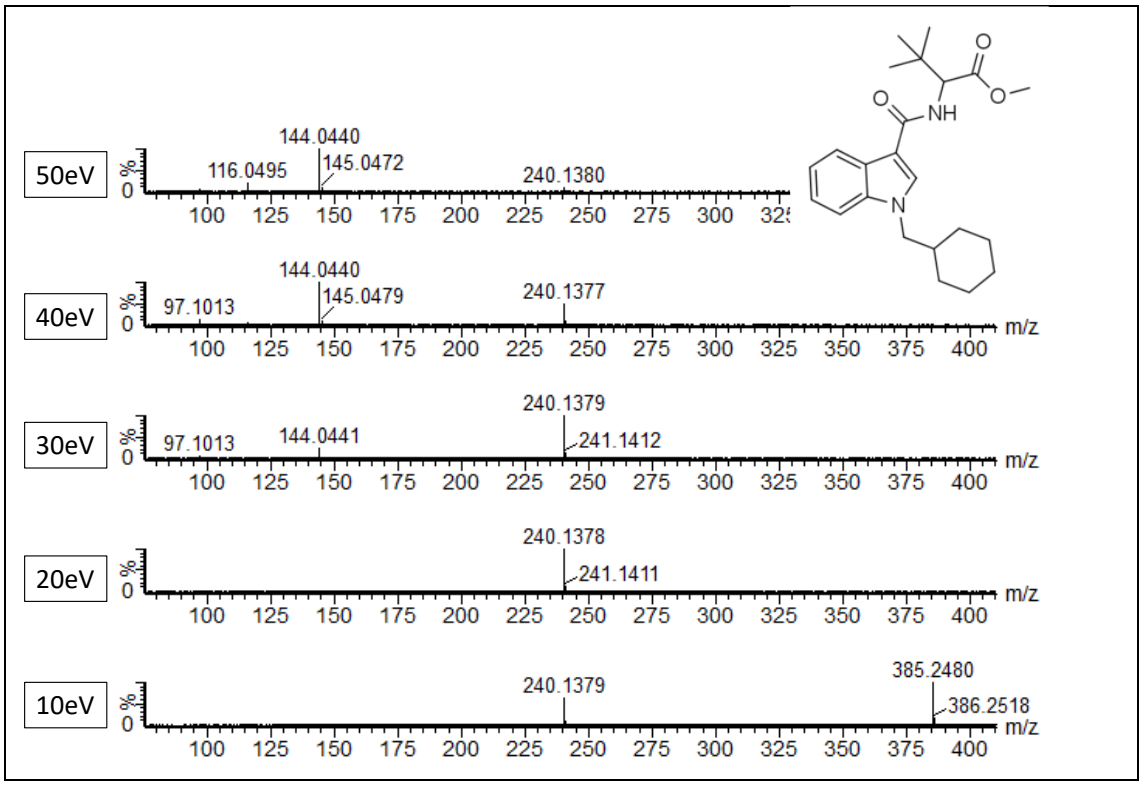

Figure S.17. UHPLC-QTOF MS/MS spectra at different collision energies (from bottom to top, 10, 20, 30, 40 and 50 eV) for MDMB-CHMICA

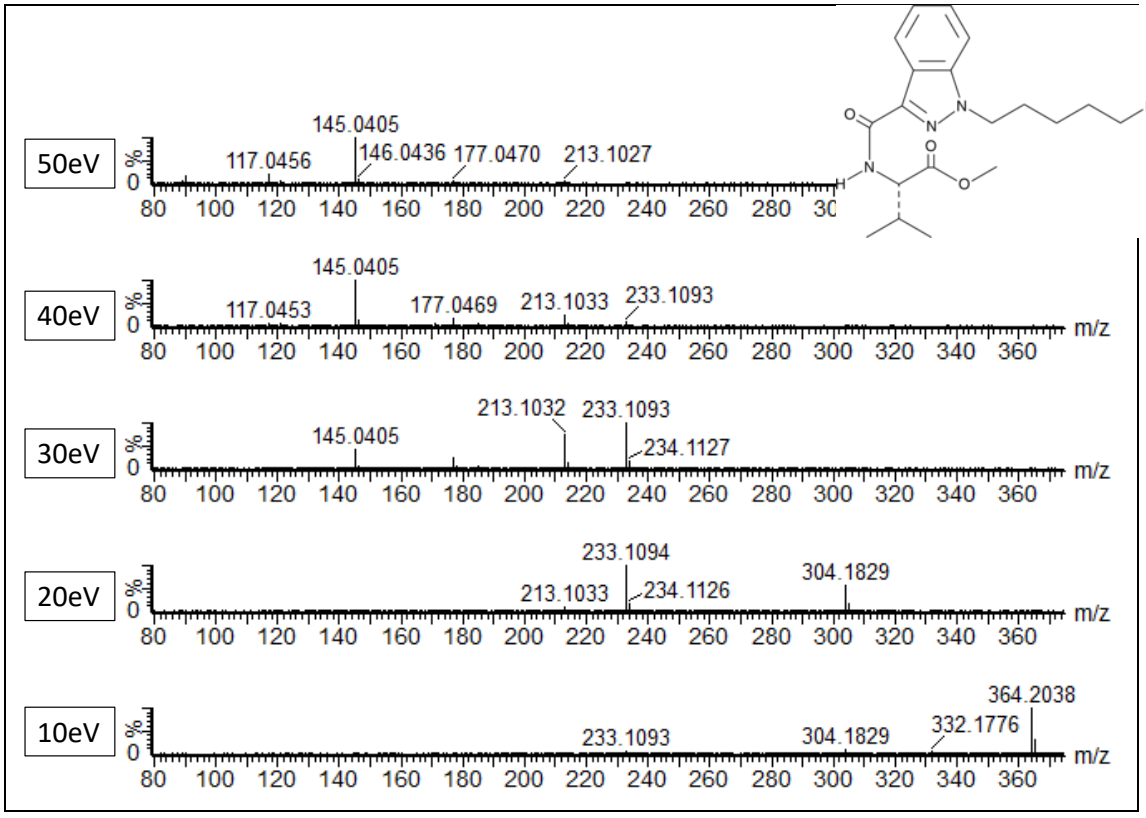

Figure S.18. UHPLC-QTOF MS/MS spectra at different collision energies (from bottom to top, 10, 20, 30, 40 and 50 eV) for 5F-AMB

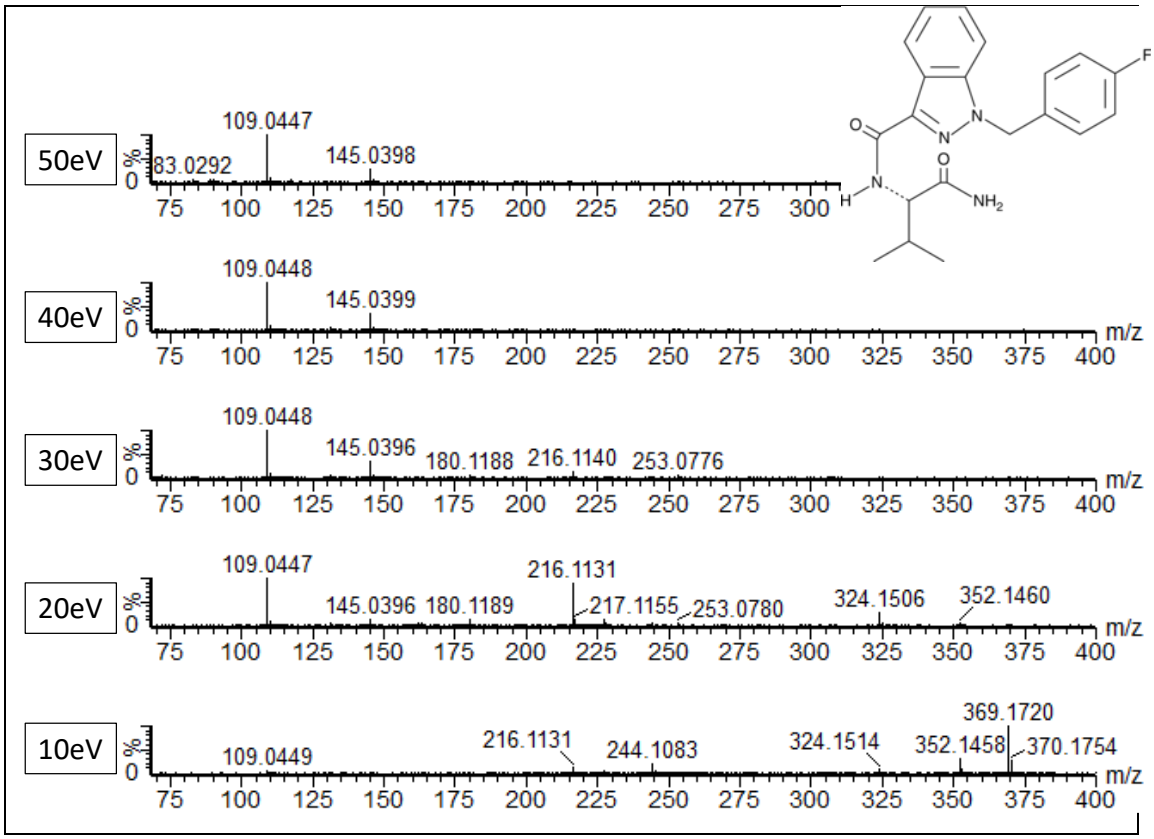

Figure S.19(a). UHPLC-QTOF MS/MS spectra at different collision energies (from bottom to top, 10, 20, 30, 40 and 50 eV) for AB-FUBINACA (11.1 min)

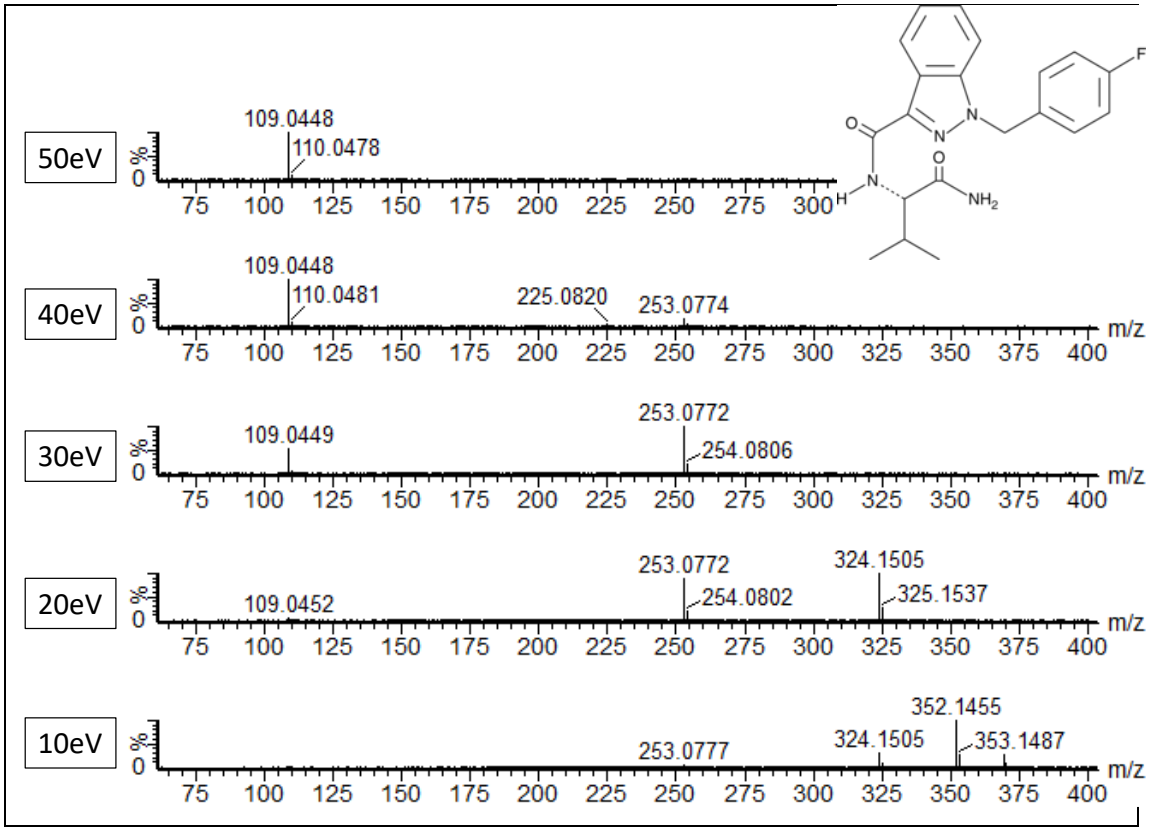

Figure S.19(b). UHPLC-QTOF MS/MS spectra at different collision energies (from bottom to top, 10, 20, 30, 40 and 50 eV) for AB-FUBINACA (11.5 min)

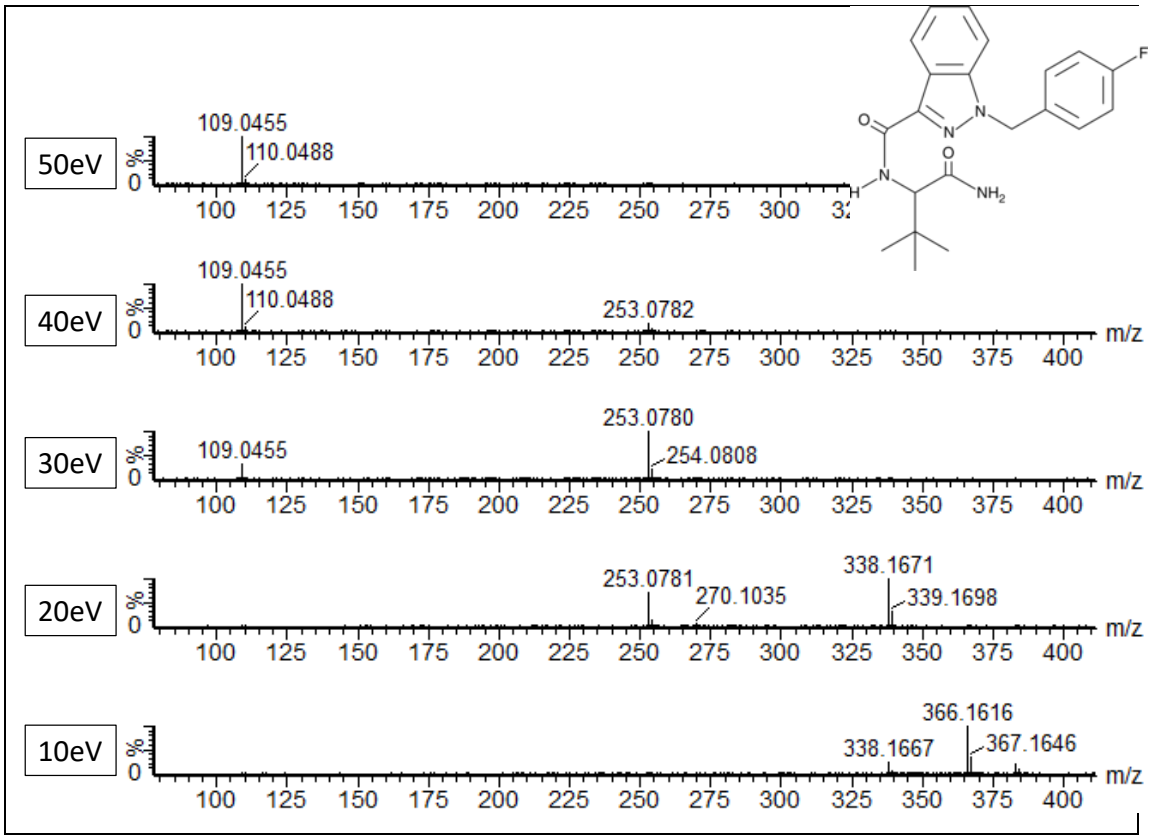

Figure S.20. UHPLC-QTOF MS/MS spectra at different collision energies (from bottom to top, 10, 20, 30, 40 and 50 eV) for ADB-FUBINACA

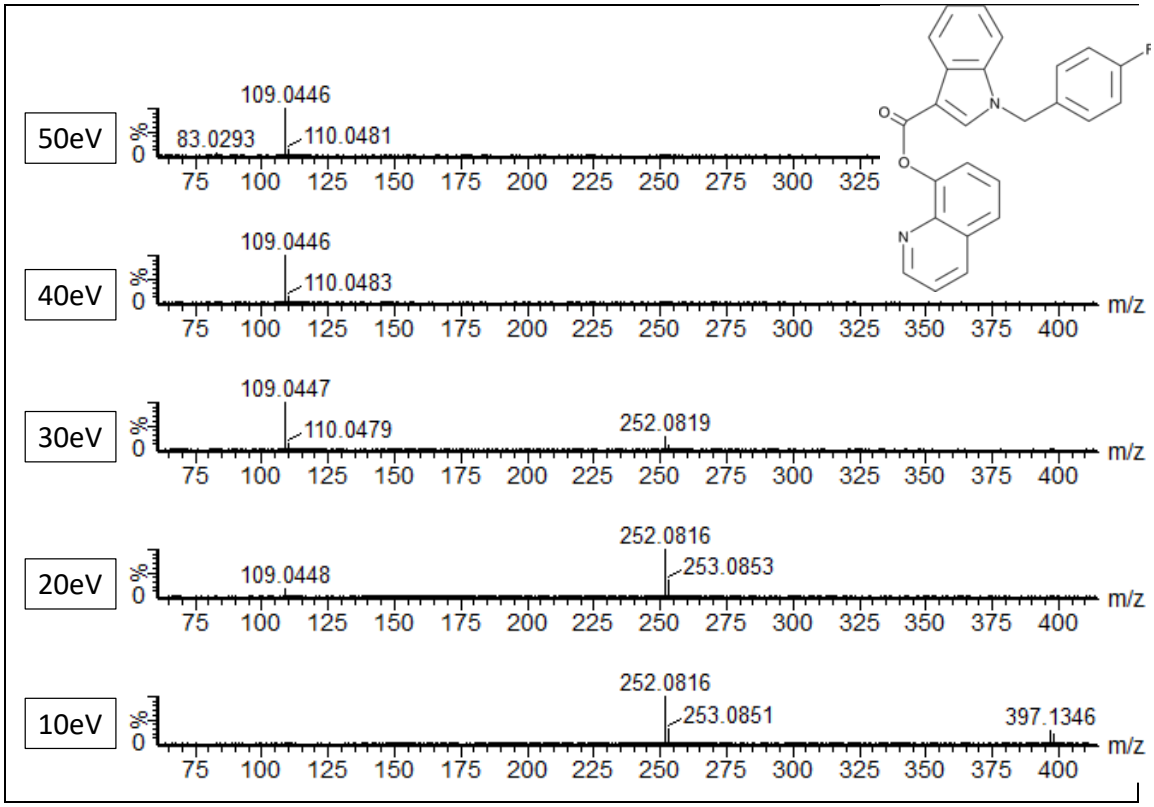

Figure S.21. UHPLC-QTOF MS/MS spectra at different collision energies (from bottom to top, 10, 20, 30, 40 and 50 eV) for FUB-PB-22

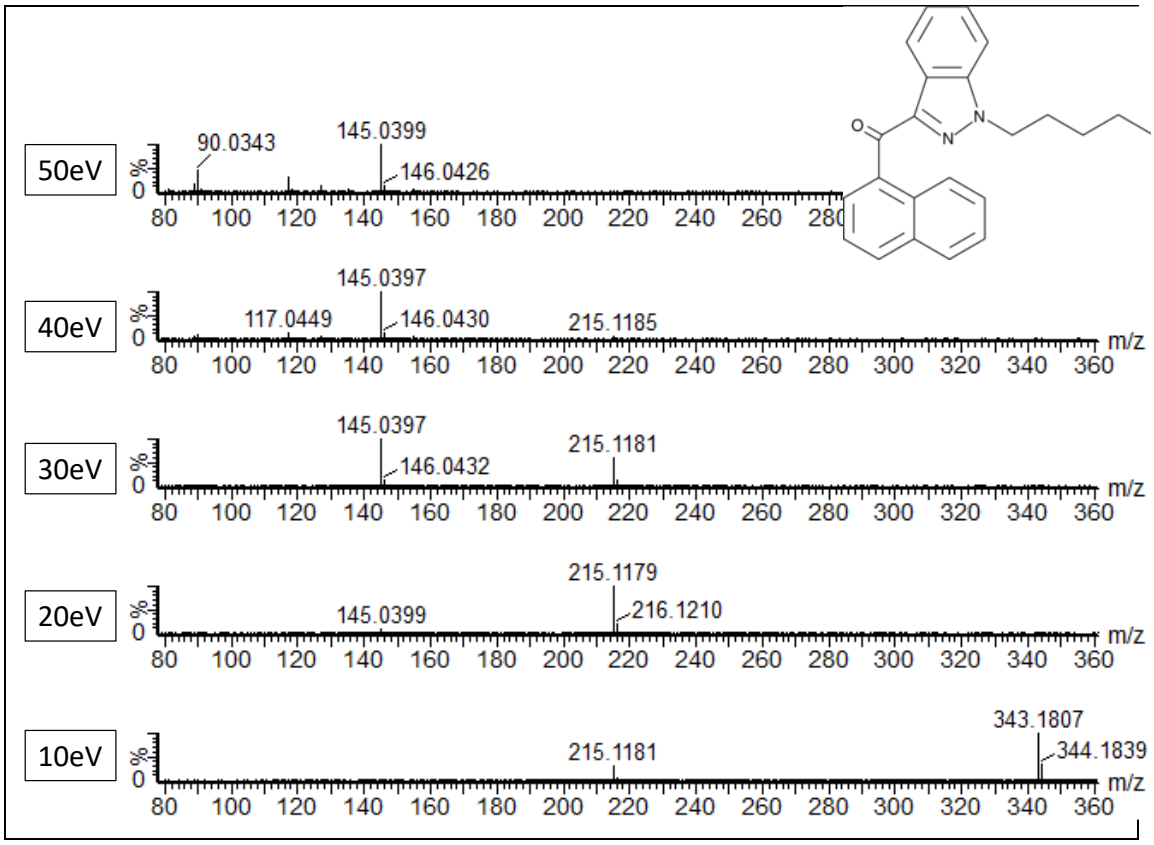

Figure S.22. UHPLC-QTOF MS/MS spectra at different collision energies (from bottom to top, 10, 20, 30, 40 and 50 eV) for THJ-018

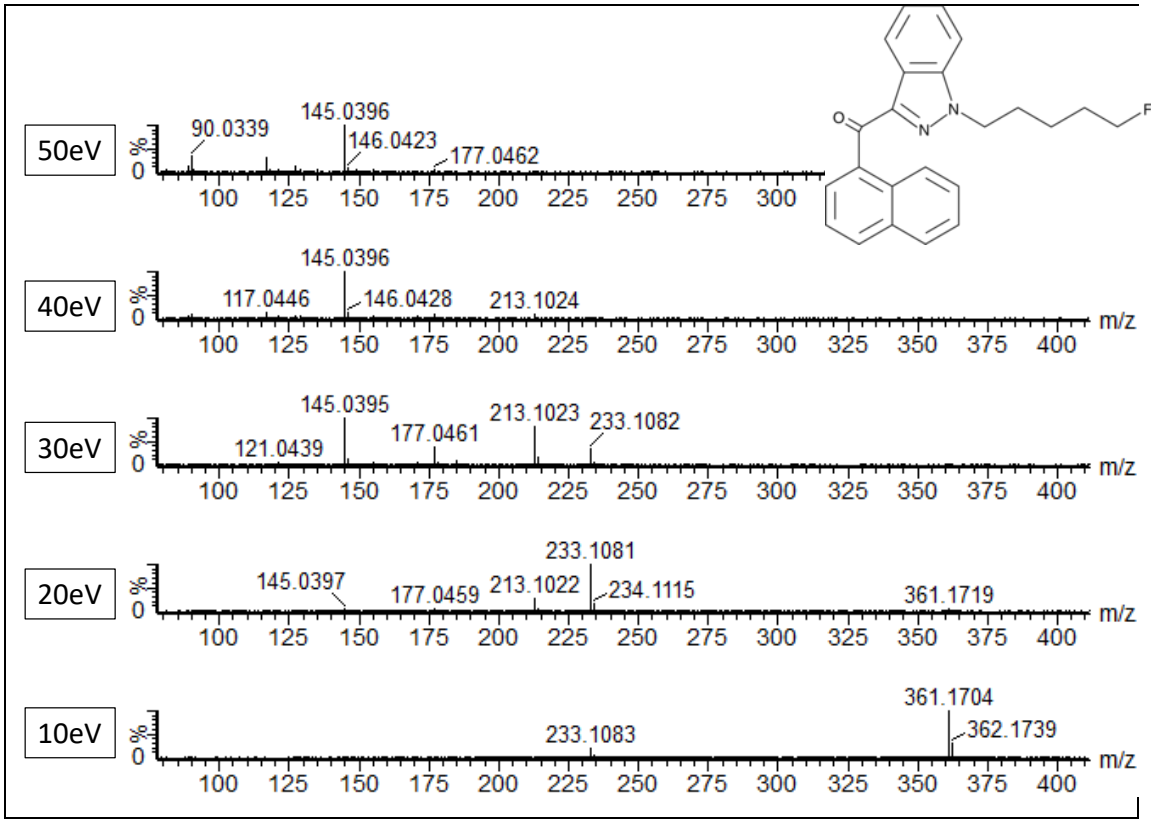

Figure S.23. UHPLC-QTOF MS/MS spectra at different collision energies (from bottom to top, 10, 20, 30, 40 and 50 eV) for THJ-2201

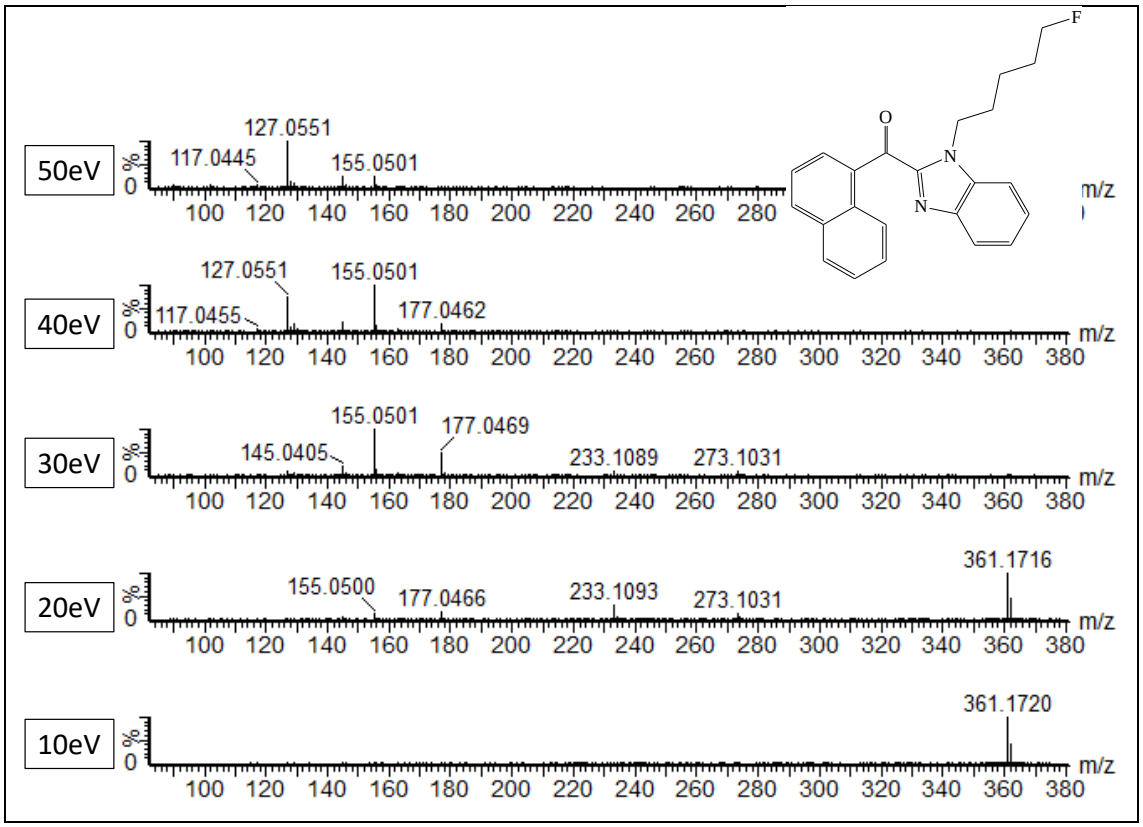

Figure S.24. UHPLC-QTOF MS/MS spectra at different collision energies (from bottom to top, 10, 20, 30, 40 and 50 eV) for BZ-2201

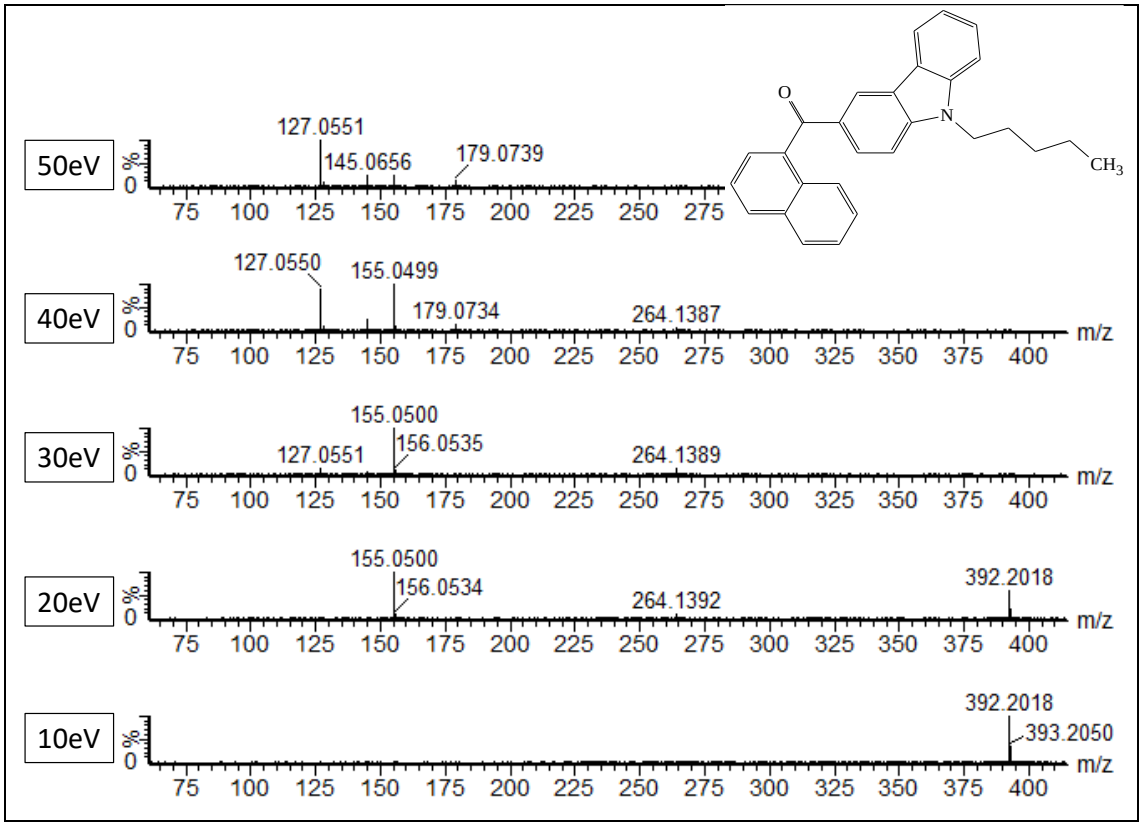

Figure S.25. UHPLC-QTOF MS/MS spectra at different collision energies (from bottom to top, 10, 20, 30, 40 and 50 eV) for EG-018